

PHASE PORTRAITS OF (2;1) REVERSIBLE VECTOR FIELDS OF LOW CODIMENSION

CLAUDIO BUZZI¹, JAUME LLIBRE² AND PAULO SANTANA¹

ABSTRACT. In this paper we study the phase portraits and bifurcation diagram of the symmetric singularities of codimensions zero, one and two of planar reversible vector fields having a line of reversibility.

1. INTRODUCTION AND MAIN RESULTS

Given two real C^k , $k \geq 1$, functions of two variables $P, Q: \mathbb{R}^2 \rightarrow \mathbb{R}$ we associate the planar C^k -differential system given by

$$(1) \quad \dot{x} = P(x, y), \quad \dot{y} = Q(x, y),$$

where the dot denotes the derivative with respect to the independent variable t . By abuse of notation we also call the map $X = (P, Q)$ a planar *vector field*. If P and Q are polynomials, then system (1) is a *planar polynomial differential system*. In this case we say that system (1) has *degree* n if the maximum of the degrees of P and Q is n . If $n = 1$, then system (1) is called a *linear differential system*. This last class of systems is already completely understood. See [31, Chapter 1].

However for $n \geq 2$ we know very few things. This class is too wide and thus it is common to study more specific subclasses and to classify their topological phase portraits. For $n = 2$ for example there is a great effort of Artes, Llibre and coauthors [2–10, 14, 22, 24, 25] to classify as many quadratic vector fields as possible.

In this paper we are concerned with the classification of the *reversible vector fields*. Let X be a C^k -vector field (not necessarily planar) and $\varphi: \mathbb{R}^m \rightarrow \mathbb{R}^m$ a C^k -diffeomorphism such that $\varphi^2 = \text{Id}_{\mathbb{R}^m}$ (also known as *involution*). Consider also

$$\text{Fix}(\varphi) = \{z \in \mathbb{R}^m : \varphi(z) = z\}.$$

We say that X is φ -reversible of type $(m; s)$ if $\text{Fix}(\varphi)$ is a sub-manifold of \mathbb{R}^m of dimension s and

$$D\varphi(z)X(z) = -X(\varphi(z)), \quad \forall z \in \mathbb{R}^m,$$

for all $z \in \mathbb{R}^m$. Many reversible vector fields have been studied for several authors. For example in [12] all the low codimension singularities of systems (2; 0)-type are classified, with their phase portraits studied at [13]. In [27] the low codimension singularities of system of (3; 2)-type are obtained. In [29, 30] there is a study of the quadratic reversible vector fields of type (3; 2) on the sphere \mathbb{S}^2 .

In this paper we study the phase portraits of the germs of C^k -reversible vector fields of type (2; 1). We recall that given a vector field X , its *germ* is the equivalence class $[X]$ given by the relation \sim defined by $X \sim Y$ if, and only if, there is a

2020 *Mathematics Subject Classification*. 34C23, 34A34, 37G10.

Key words and phrases. Reversibility; phase portrait; reversible vector fields; codimension one; codimension two.

neighborhood U of the origin such that X and Y coincide in U . By abuse of notation we denote the germ of X also by X .

Let $\mathbb{R}^2, 0$ denote plane coordinates in a neighborhood of the origin. Given a φ -reversible vector field of type $(2; 1)$, it is well known that we can choose a coordinate system at $\mathbb{R}^2, 0$ such that $\varphi(x, y) = (x, -y)$, see Appendix A.

Therefore let \mathfrak{X} denote the set of germs of reversible vector fields of type $(2; 1)$ at $\mathbb{R}^2, 0$ endowed with the C^k -topology and observe that given $X \in \mathfrak{X}$, it is no loss of generality to assume that X is φ -reversible with $\varphi(x, y) = (x, -y)$.

Definition 1 (Topological equivalence). *Two germs of vector fields $X, Y \in \mathfrak{X}$ are topologically equivalent if there are two neighborhoods U, V of the origin and a homeomorphism $h: U \rightarrow V$ which sends orbits of X to orbits of Y preserving or reversing the orientation of all orbits. The homeomorphism h is called a topological equivalence between X and Y . Moreover we say that $X \in \mathfrak{X}$ is structurally stable if there is a neighborhood $N \subset \mathfrak{X}$ of X such that X is topologically equivalent to every $Y \in N$.*

Let $\Sigma_0 \subset \mathfrak{X}$ be the family of structurally stable germs and consider the codimension one bifurcation set $\mathfrak{X}_1 = \mathfrak{X} \setminus \Sigma_0$, endowed with the subspace topology induced by \mathfrak{X} . Let $\Sigma_1 \subset \mathfrak{X}_1$ be the family of structurally stable germs relatively to \mathfrak{X}_1 and consider the codimension two bifurcation set $\mathfrak{X}_2 = \mathfrak{X}_1 \setminus \Sigma_1$. Finally, let $\Sigma_2 \subset \mathfrak{X}_2$ be the family of structurally stable germs relatively to \mathfrak{X}_2 .

Definition 2 (k -parameter families). *Given $k \in \{1, 2\}$ let Θ_k be the space of C^1 -mappings $\xi: \mathbb{R}^k \rightarrow \mathfrak{X}$ endowed with the C^1 -topology. Its elements ξ are called k -parameter families of germs of vector fields of \mathfrak{X} . Given $\xi \in \Theta_k$ and $\lambda \in \mathbb{R}^k$, we say that the germ of vector field $\xi(\lambda) \in \mathfrak{X}$ is an element of the family ξ .*

In the following theorem Teixeira [36] provided a characterization of the normal forms of the elements of Σ_0 and also for dense sets of Φ_1 and Φ_2 .

Theorem 1 (Teixeira [36]). *The following statements hold.*

- (a) (Codimension zero classification) *If $X \in \Sigma_0$, then it is topologically equivalent to one of the following germs of vector fields.*
 1. $X_{01} = (0, \frac{1}{2})$.
 2. $X_{02} = (y, \delta x)$, $\delta \in \{-1, 1\}$.
- (b) (Codimension one classification) *In Θ_1 a dense set is formed by the families whose each element is topologically equivalent to one of the elements of the following families.*
 1. *The normal forms of item (a).*
 2. $X_{11} = (y, \frac{1}{2}(\lambda + x^2))$.
 3. $X_{12} = (\delta xy, \frac{1}{2}(2\delta y^2 + x + \lambda))$, $\delta \in \{-1, 1\}$.
 4. $X_{13} = (xy, \frac{1}{2}(-y^2 + x + \lambda))$.
 5. $X_{14} = (xy + y^3, \frac{1}{2}(-x + y^2 + \lambda))$.
- (c) (Codimension two classification) *In Θ_2 a dense set is formed by the families whose each element is topologically equivalent to one of the elements of the following families.*
 1. *All the normal forms listed item (b).*
 2. $X_{21} = (y, \frac{1}{2}(bx^3 + \beta x + \alpha))$, $b \in \{-1, 1\}$.
 3. (i) $X_{22a} = (ay(x - y^2) + \beta y(x + y^2), \frac{1}{2}(\alpha + (x + y^2)^2))$, $a \in \{-1, 1\}$.
(ii) $X_{22b} = (y(x - y^2) + \beta y(x + y^2), \frac{1}{2}(\alpha + a(x + y^2)^2))$, $a \in \{-1, 1\}$.

4. $X_{23} = (-y^3 + axy(\alpha + x^2 + y^4), \frac{1}{2}(ax - y^2(\alpha + x^2 + y^4) + \beta))$, $a \in \{-1, 1\}$.
5. $X_{24} = (axy + \alpha y^3, \frac{1}{2}(x + ay^2 + \beta))$, $a \in \{-1, 1\}$.
6. (i) $X_{25a} = (xy, \frac{1}{2}(\alpha x - y^2 + ax^2 + \beta))$, $a \in \{-1, 1\}$.
 (ii) $X_{25b} = (axy, \frac{1}{2}(\alpha x + by^2 + \delta x^2 + \beta))$, $ab > 0$, $\delta \in \{-3, 3\}$ and $\{(a \in \{-1, 1\}, b \in \{-3, 3\}) \text{ or } (a \in \{-3, 3\}, b \in \{-1, 1\})\}$.

The families X_{ij} that appears at Theorem 1(b) and (c) are the topological normal forms that characterizes all possible ways to cross Σ_1 and Σ_2 transversely in the space \mathfrak{X} of all germs. In particular the dense set of families stated at Theorem 1 are those characterized by the fact that whenever it crosses \mathfrak{X}_k , then it does transversely and at structurally stable elements.

We note that such families are polynomial and thus we are motivated to obtain the bifurcation diagrams and the phase portraits of such vector fields in order to complement the results of Teixeira [36]. Therefore our first main result is the following.

Theorem A. *The bifurcation diagram and the phase portraits in the Poincaré disk of the vector fields in Theorem 1 are given in Figures 19-36.*

We observe that the bifurcation diagram and phase portraits presented at Theorem A are *global* and defined for all values of $\lambda \in \mathbb{R}$ and $(\alpha, \beta) \in \mathbb{R}^2$.

Definition 3. *Let X be a φ -reversible vector field of type $(m; s)$. We say that p is a symmetric singularity of X if $\varphi(p) = p$.*

It follows from [36] that the families X_{ij} that appear at Theorem 1(b) and (c) are also the topological normal forms of the symmetric singularities of codimension one and two.

Therefore we observe that if we restrict the phase portraits of Theorem A to a neighborhood of the origin and for $\lambda \approx 0$ or $(\alpha, \beta) \approx (0, 0)$, then we have a characterization of the local phase portraits of the symmetric singularities of low codimension of reversible vector fields of type (2; 1). Therefore our second main result is the following.

Theorem B. *A symmetric singularity of codimension zero, one or two of a reversible vector field of type (2; 1) is topologically equivalent to one of the phase portraits given in Figures 19-36, at the origin and for $\lambda \approx 0$ or $(\alpha, \beta) \approx (0, 0)$.*

We observe that the phase portraits given in Figures 19-36 does not represent the global phase portraits of all reversible vector fields of type (2; 1) of low codimension. In fact, unless we are given a maximum degree, a reversible vector field of type (2; 1) may have as many singularities as desired and thus there is infinitely many of such phase portraits. For a classification of all the phase portraits of the quadratic reversible vector fields of type (2; 1) we refer to [23].

Remark 1. *The phase portraits work as follows. The thicker lines represent the separatrices of the phase portrait and the thin lines represent generic orbits of the canonical regions (see Appendix D). The bigger dots represent isolated singularities. The dotted line at some phase portraits of the bifurcation diagram of X_{12} and X_{24a} represents a line of singularities. Moreover if a phase portrait at the bifurcation diagram has no pointing lines, then it represents the open connected region in which it is inserted.*

Remark 2. For simplicity we call the origin of the charts U_2 , V_2 , U_1 and V_1 of the Poincaré compactification (see Appendix B) as north pole, south pole, east pole and west pole, respectively.

The paper is organized as follows. In Section 2 we present the backbone of the approaching method. In Sections 3-6 we study the main peculiarities of the families of codimension two. In the Appendix we have a brief survey on some technical results used in the proves of our results.

2. APPROACHING METHOD

The backbone of our approach is first to study all the local phase portrait at every finite singularity and at the infinity (see Appendix B), then to discover when it may exist some limit cycle and finally to study when it may happen some bifurcation as the saddle-node, the center-focus, Hopf bifurcation and etc. After this we study the α and ω -limits of all the separatrices (see Appendix D). To do this we use some convenient straight lines and curves to see at which direction the flow crosses it.

Let us take system X_{12} as an example. We remember it is given by

$$\dot{x} = \delta xy, \quad \dot{y} = \frac{1}{2} (2\delta y^2 + x + \lambda),$$

with $\delta \in \{-1, 1\}$. First we observe that if $\delta = -1$, then with the change of variables and parameter $(x, y; \lambda) \mapsto (-x_1, -y_1; -\lambda_1)$ we return to the case $\delta = 1$ and thus both cases are equivalent. Therefore it is no loss of generality to assume $\delta = 1$. Moreover we observe that the only possible finite singularities are given by

$$p = (-\lambda, 0), \quad q^\pm = \pm \left(0, \sqrt{-\frac{\lambda}{2}} \right).$$

Therefore as anticipated in the begining of this section, our first step is to obtain the local phase portraits at the finite singularities of X_{12} .

Proposition 1. *The following statements hold.*

- (a) p is a hyperbolic saddle if $\lambda < 0$ and a center if $\lambda > 0$.
- (b) q^+ (resp. q^-) is a unstable node (resp. stable node) if $\lambda < 0$.
- (c) The origin is the unique finite singularity if $\lambda = 0$ and its phase portrait is given by Figure 1.
- (d) X_{12} does not have limit cycles.

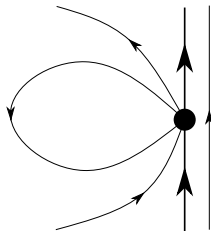


FIGURE 1. Local phase portrait of X_{12} at the origin with $\lambda = 0$.

Proof. Knowing that a symmetric singularity cannot be a focus (see [37, Section 2]), statements (a) and (b) follows from the linear parts of X_{12} at the singularities p and q^\pm ,

$$DX_{12}(p) = \begin{pmatrix} 0 & -\lambda \\ \frac{1}{2} & 0 \end{pmatrix}, \quad DX_{12}(q^\pm) = \pm \begin{pmatrix} \frac{1}{\sqrt{2}}\sqrt{-\lambda} & 0 \\ \star & \sqrt{2}\sqrt{-\lambda} \end{pmatrix},$$

in addition with the Stable Manifold Theorem, see [31, Sec 2.7].

Doing a quasihomogeneous blow up at the origin when $\lambda = 0$ with weights $(\alpha, \beta) = (2, 1)$ (see Appendix C), we obtain the vector field $X_0 = X_0(r, \theta)$ given by,

$$\dot{r} = rR_1(r, \theta), \quad \dot{\theta} = \cos \theta (\cos \theta + \sin^2 \theta) + rR_2(r, \theta).$$

Therefore the singularities of X_0 such that $r = 0$ are given by $\theta \in \{\pm\frac{1}{2}\pi, \theta^\pm\}$, where $\theta^\pm = \pm \arccos(\frac{1}{2}(1 - \sqrt{5}))$. Hence statement (c) follows from

$$DX_0(0, \pm\frac{\pi}{2}) = \pm \begin{pmatrix} 1 & 0 \\ 0 & -1 \end{pmatrix},$$

$$DX_0(0, \theta^\pm) = \pm \begin{pmatrix} \frac{1}{2}\sqrt{5(\sqrt{5}-2)} & 0 \\ 0 & \sqrt{5(\sqrt{5}-2)} \end{pmatrix}.$$

Statement (d) follows from the invariance of the y -axis and the fact that a limit cycle cannot surround only a unique saddle, see Appendix E. \square

Now the next step is to find the local phase portrait at the infinity of the Poincaré compactification of X_{12} , see Appendix B.

Proposition 2. *The infinity of X_{12} is filled up of singularities and its local phase portrait is given by Figure 2.*

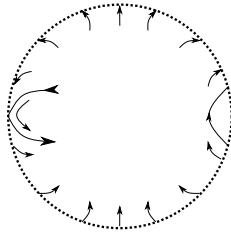


FIGURE 2. Local phase portrait at the infinity of X_{12} .

Proof. In the chart U_1 of the Poincaré compactification system X_{12} becomes

$$\dot{u} = \frac{1}{2}v + \frac{\lambda}{2}v^2, \quad \dot{v} = -uv.$$

And in the chart U_2 we have

$$\dot{u} = -\frac{1}{2}u^2v - \frac{\lambda}{2}uv^2, \quad \dot{v} = -v - \frac{1}{2}uv^2 - \frac{\lambda}{2}v^3.$$

Therefore we conclude that the infinity is filled up of singularities. Doing a regularization in v , i.e. dividing both systems by v , one can see that the flow of the

regularized system at $v = 0$ is given by Figure 3. More precisely, let $X = X(u, v)$ be the regularized version of system X_{12} at the chart U_1 , i.e. X is given by

$$\dot{u} = \frac{1}{2} + \frac{\lambda}{2}v, \quad \dot{v} = -u.$$

Let $h(u, v) = v$, $Xh(p) = \langle X(p), \nabla h(p) \rangle$ and $X^n h(p) = \langle X(p), \nabla X^{n-1} h(p) \rangle$, where $\langle \cdot, \cdot \rangle$ denotes the standard inner product of \mathbb{R}^2 . One can conclude that $h(0, 0) = Xh(0, 0) = 0$, $X^2 h(0, 0) = -\frac{1}{2}$, and thus obtain Figure 3. \square

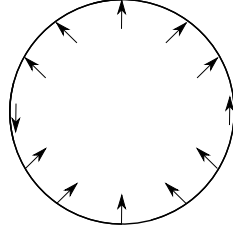


FIGURE 3. Local phase portrait of the regularized infinity of X_{12} .

Now we have the local behavior of X_{12} in all its singularities and we know that it does not have limit cycles. Hence we can start working on its separatrices.

Proposition 3. *The phase portrait of X_{12} for $\lambda < 0$ is the one given in Figure 19.*

Proof. From Propositions 1 and 2 we conclude Figure 4. First we observe that the

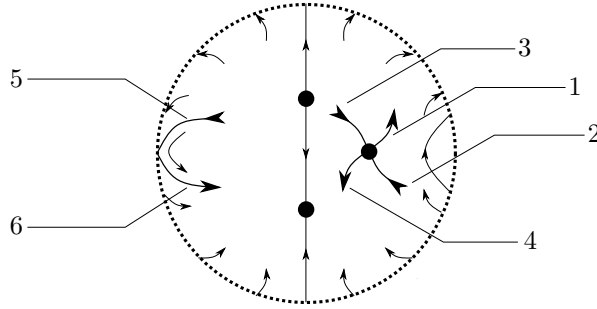


FIGURE 4. Local behavior of the phase portrait of X_{12} for $\lambda < 0$.

flow crosses the x -axis downwards if $x < -\lambda$ and upwards if $x > -\lambda$. Therefore, separatrix 4 cannot cross the x -axis, otherwise separatrix 2 would have no α -limit. Hence, separatrix 4 has no other option than ending at the stable node q^- . By symmetry separatrix 3 borns at the unstable node. Now separatrix 1 has no other option than ending at some singularity of the first quadrant of the infinity and thus separatrix 2 borns at the symmetric singularity at the fourth quadrant. Clearly separatrix 6 has no option than ending at the stable node and therefore separatrix 5 borns at the unstable node. \square

Proposition 4. *The phase portrait of X_{12} for $\lambda = 0$ is the one given in Figure 19.*

Proof. From Propositions 1 and 2 we conclude Figure 5. We know that the flow

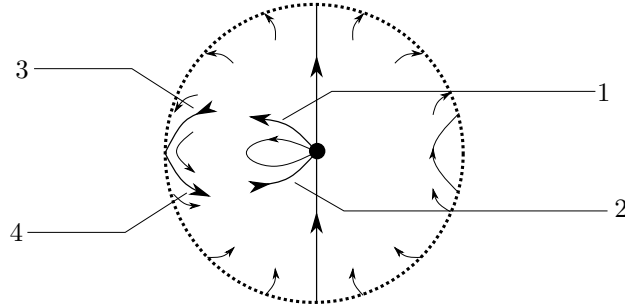


FIGURE 5. Local behavior of the phase portrait of X_{12} for $\lambda = 0$.

crosses the x -axis downwards if $x < 0$, therefore separatrix 4 has no other option than glue up to separatrix 2 and thus by symmetry separatrix 1 glues up to separatrix 3. \square

Proposition 5. *The phase portrait of X_{12} for $\lambda > 0$ is the one given in Figure 19.*

Proof. From Propositions 1 and 2 we conclude Figure 6. Here we just need to

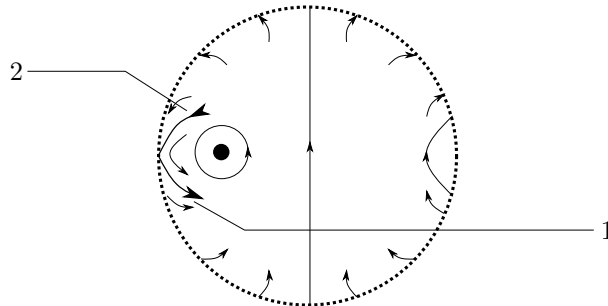


FIGURE 6. Local behavior of the phase portrait of X_{12} for $\lambda > 0$.

observe that separatrix 1 must cross the x -axis and thus by symmetry it must glue to separatrix 2. \square

With this same approach one can also conclude the phase portraits of X_{01} , X_{02} , X_{11} , X_{13} and X_{14} .

Before we study the systems of codimension 2 we must know when they are topologically equivalent, at some finite singularity, to the origin of X_{11} , X_{12} , X_{13} or X_{14} , for $\lambda \approx 0$. To this end we use a characterization provided by Teixeira [36].

Let $h: \mathbb{R}^2 \rightarrow \mathbb{R}$ be given by $h(x, y) = y$ and recall that the n -th Lie derivative of h at p in the direction of a vector field X is given by,

$$Xh(p) = \langle X(p), \nabla h(p) \rangle, \quad X^n h(p) = \langle X(p), \nabla X^{n-1} h(p) \rangle,$$

where $\langle \cdot, \cdot \rangle$ denotes the standard inner product of \mathbb{R}^2 .

Definition 4. Let p be a symmetric singularity (S -singularity, for short) of $X \in \mathfrak{X}$. We say that p is a:

- (a) cusp S -singularity if $h(p) = Xh(p) = X^2h(p) = 0$ and $X^3h(p) \neq 0$.
- (b) nodal S -singularity if $X(p) = 0$, the eigenvalues λ_1 and λ_2 of $DX(p)$ are real, distinct, $\lambda_1\lambda_2 > 0$ and its eigenspaces are transverse to $y = 0$ at p .
- (c) saddle S -singularity if $X(p) = 0$, the eigenvalues λ_1 and λ_2 of $DX(p)$ are real, distinct, $\lambda_1\lambda_2 < 0$ and its eigenspaces are transverse to $y = 0$ at p .
- (d) focal S -singularity if p is a hyperbolic singularity of X and the eigenvalues of $DX(p)$ are given by $\lambda = a + ib$ with $b \neq 0$.

It follows from Lemma 4.2 of [36] that if p is a cusp, nodal, saddle or focal S -singularity, then X is locally topologically equivalent at p to the origin of X_{11} , X_{12} , X_{13} or X_{14} , respectively, for $\lambda \approx 0$.

3. SYSTEM X_{21}

Let us remember that system X_{21} is given by

$$\dot{x} = y, \quad \dot{y} = \frac{1}{2}(bx^3 + \beta x + \alpha),$$

with $b \in \{-1, 1\}$. From now on we assume $b = 1$. Clearly the finite singularities of X_{21} are given by $(x_0, 0)$, where x_0 is a real root of the polynomial $p(x) = x^3 + \beta x + \alpha$. Following the Cardano-Tartaglia formula (see Appendix F) we define $D = \frac{1}{27}\beta^3 + \frac{1}{4}\alpha^2$ and observe that $D = 0$ if, and only if, $\beta = \beta(\alpha)$ where

$$\beta(\alpha) = -\frac{3}{\sqrt[3]{4}}\sqrt[3]{\alpha^2}.$$

Therefore from Appendix F we conclude the following statements.

- (a) If $\beta > \beta(\alpha)$ we have a unique finite singularity.
- (b) If $\beta < \beta(\alpha)$ we have three finite singularities.
- (c) If $\beta = \beta(\alpha)$ and $\alpha \neq 0$ we have two finite singularities.
- (d) If $\beta = \beta(\alpha)$ and $\alpha = 0$, then the origin is the unique finite singularity.

From Appendix F we have that we can denote the zeros of $p(x) = 0$ by

$$\begin{aligned} x_1 &= S + T, \\ x_2 &= -\frac{1}{2}(S + T) + \frac{1}{2}\sqrt{3}(S - T)i, \\ x_3 &= -\frac{1}{2}(S + T) - \frac{1}{2}\sqrt{3}(S - T)i, \end{aligned}$$

where $i^2 = -1$ and

$$S = f\left(-\frac{\alpha}{2} + D^{\frac{1}{2}}\right), \quad T = f\left(-\frac{\alpha}{2} - D^{\frac{1}{2}}\right), \quad f(x) = \begin{cases} \sqrt[3]{x}, & \text{if } D \geq 0, \\ x^{\frac{1}{3}}, & \text{if } D < 0. \end{cases}$$

With this machinery we can now study the relative position of the real solutions of the polynomial $p(x) = x^3 + \beta x + \alpha$.

Proposition 6. *The relative position of the real solutions of p is the following.*

- (a) If $D < 0$ then $x_2 < x_3 < x_1$.
- (b) If $D = 0$ and $\alpha < 0$, then $x_2 = x_3 < x_1$.
- (c) If $D = 0$ and $\alpha > 0$, then $x_1 < x_2 = x_3$.
- (d) Otherwise x_1 is the unique real solution.

Proof. We start with statement (a), which we separate in three parts. If $D < 0$ and $\alpha < 0$, then $S = (a + ib)^{\frac{1}{3}}$, where $a = -\frac{1}{2}\alpha > 0$ and $b = \sqrt{-D} > 0$. Therefore if we denote $r = \sqrt{a^2 + b^2}$ and $\theta = \frac{1}{3} \arctan\left(\frac{b}{a}\right)$ we obtain $S = \sqrt{-\frac{\beta}{3}}(\cos \theta + i \sin \theta)$. In a similar way one can see that $T = \sqrt{-\frac{\beta}{3}}(\cos \theta - i \sin \theta)$. Hence,

$$\begin{aligned} x_1 &= 2\sqrt{-\frac{\beta}{3}} \cos \theta, \\ x_2 &= -\sqrt{-\frac{\beta}{3}}(\cos \theta + \sqrt{3} \sin \theta), \\ x_3 &= -\sqrt{-\frac{\beta}{3}}(\cos \theta - \sqrt{3} \sin \theta). \end{aligned}$$

Observe that

$$\frac{b}{a} = \frac{\sqrt{-D}}{-\frac{1}{2}\alpha} = -\frac{2}{\alpha} \sqrt{-\frac{\beta^3}{27} - \frac{\alpha^2}{4}} = \frac{2}{|\alpha|} \sqrt{-\frac{\beta^3}{27} - \frac{\alpha^2}{4}} = \sqrt{\frac{4}{27} \frac{(-\beta)^3}{\alpha^2} - 1}.$$

Given $\beta_0 < 0$ fixed we know that $\alpha \in (\alpha(\beta_0), 0)$, where $\alpha(\beta) = -\sqrt{-\frac{4}{27}\beta^3}$. Similarly, given $\alpha_0 < 0$ fixed we know that $\beta \in (-\infty, \beta(\alpha))$. Therefore we have that $\theta = \theta(\alpha, \beta) \in (0, \frac{1}{6}\pi)$ and

$$\lim_{D \rightarrow 0} \theta(\alpha, \beta) = 0, \quad \lim_{\beta \rightarrow -\infty} \theta(\alpha_0, \beta) = \lim_{\alpha \rightarrow 0} \theta(\alpha, \beta_0) = \frac{\pi}{6}.$$

Hence we conclude that in this case we have $x_2 < x_3 < 0 < x_1$ and also,

$$\lim_{D \rightarrow 0} |x_2 - x_3| = 0, \quad \lim_{\beta \rightarrow -\infty} x_3(\alpha_0, \beta) = \lim_{\alpha \rightarrow 0} x_3(\alpha, \beta_0) = 0.$$

If $D < 0$ and $\alpha > 0$ we have

$$\begin{aligned} x_1 &= 2\sqrt{-\frac{\beta}{3}} \cos \theta, \\ x_2 &= -\sqrt{-\frac{\beta}{3}}(\cos \theta + \sqrt{3} \sin \theta), \\ x_3 &= -\sqrt{-\frac{\beta}{3}}(\cos \theta - \sqrt{3} \sin \theta), \end{aligned}$$

where $\theta = \frac{1}{3} \arctan\left(-\frac{2}{\alpha} \sqrt{-D}\right) + \frac{1}{3}\pi$. Since we have $\alpha > 0$ it follows that

$$-\frac{2}{\alpha} \sqrt{-D} = -\sqrt{\frac{4}{27} \frac{(-\beta)^3}{\alpha^2} - 1}.$$

Given $\beta_0 < 0$ fixed we know that $\alpha \in (0, \alpha(\beta_0))$, where $\alpha(\beta) = \sqrt{-\frac{4}{27}\beta^3}$. Similarly, given $\alpha_0 > 0$ fixed we know that $\beta \in (-\infty, \beta(\alpha))$. Therefore it follows that $\theta = \theta(\alpha, \beta) \in (\frac{1}{6}\pi, \frac{1}{3}\pi)$ and

$$\lim_{D \rightarrow 0} \theta(\alpha, \beta) = \frac{\pi}{3}, \quad \lim_{\beta \rightarrow -\infty} \theta(\alpha_0, \beta) = \lim_{\alpha \rightarrow 0} \theta(\alpha, \beta_0) = \frac{\pi}{6}.$$

Hence we conclude that in this case we have $x_2 < 0 < x_3 < x_1$ and also,

$$\lim_{D \rightarrow 0} |x_1 - x_3| = 0, \quad \lim_{\beta \rightarrow -\infty} x_3(\alpha_0, \beta) = \lim_{\alpha \rightarrow 0} x_3(\alpha, \beta_0) = 0.$$

If $D < 0$ and $\alpha = 0$, then

$$S = \frac{1}{2} \sqrt{-\frac{\beta}{3}} (\sqrt{3} + i), \quad T = \frac{1}{2} \sqrt{-\frac{\beta}{3}} (\sqrt{3} - i),$$

and thus

$$x_1 = \sqrt{-\beta}, \quad x_2 = -\sqrt{-\beta}, \quad x_3 = 0.$$

Moreover, observe that in this case we have

$$\lim_{D \rightarrow 0} x_1(\alpha, \beta) = \lim_{D \rightarrow 0} x_2(\alpha, \beta) = 0.$$

Hence one can conclude statement (a).

If $D = 0$ then $S = T = \sqrt[3]{-\frac{1}{2}\alpha}$ and thus

$$(2) \quad x_1 = 2\sqrt[3]{-\frac{1}{2}\alpha}, \quad x_2 = x_3 = \sqrt[3]{\frac{1}{2}\alpha}.$$

Statements (b) and (c) follow from (2) if $\alpha \neq 0$. If $\alpha = 0$ one obtain $x_1 = x_2 = x_3$ as in statement (d).

Finally if $D > 0$ or $D = \alpha = 0$, then the unique real zero is given by

$$x_1 = \sqrt[3]{-\frac{\alpha}{2} + \sqrt{D}} + \sqrt[3]{-\frac{\alpha}{2} - \sqrt{D}},$$

as in statement (d). □

Now that we have information about the real roots of $p(x) = x^3 + \beta x + \alpha$ we study the phase portraits of the singularities of X_{21} .

Proposition 7. *Let $p_i = (x_i, 0)$, $i \in \{1, 2, 3\}$ be the singularities of X_{21} . The local phase portraits of X_{21} at these singularities are the following.*

- (a) *If $D > 0$, then p_1 is a saddle.*
- (b) *If $D < 0$, then p_1 and p_2 are saddles and p_3 is a center.*
- (c) *If $D = 0$ and $\alpha \neq 0$, then p_1 is a saddle and $p_2 = p_3$ is a cusp, as in Figure 7.*
- (d) *If $D = \alpha = 0$, then p_1 is a non-hyperbolic saddle.*

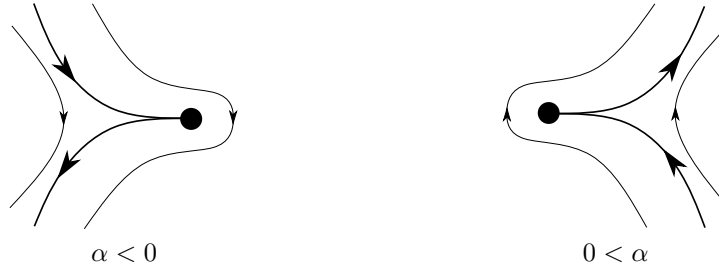


FIGURE 7. Local phase portrait of X_{21} at $p_2 = p_3$ when $D = 0$.

Proof. Observe that the Jacobian matrix at a singularity p_i is given by

$$DX_{21}(p_i) = \begin{pmatrix} 0 & 1 \\ \frac{1}{2}\beta + \frac{3}{2}x_i^2 & 0 \end{pmatrix}.$$

We first work statement (a). In this case p_1 is the unique finite singularity. Clearly it is a saddle if $\beta \geq 0$. If $\beta < 0$ then

$$\frac{1}{2}\beta + \frac{3}{2}x_1^2 = \frac{3}{2}(S^2 + T^2) - \frac{1}{2}\beta > 0,$$

with the last inequality due to the fact that $\beta < 0$. In particular if $\beta < 0$ then p_1 is still a saddle.

Let us now work statement (b). Since $\beta < 0$ is a necessary conditions for D , we have that

$$\frac{1}{2}\beta + \frac{3}{2}x_1^2 = -\beta \left(2\cos^2\theta - \frac{1}{2} \right) > 0.$$

Therefore p_1 is a hyperbolic saddle. Observe now that

$$\frac{1}{2}\beta + \frac{3}{2}x_2^2 = -\beta \sin\theta(\sin\theta + \sqrt{3}\cos\theta) > 0,$$

because $\beta < 0$ and $\theta \in (0, \frac{1}{3}\pi)$. Therefore, p_2 is also a hyperbolic saddle. Finally,

$$\frac{1}{2}\beta + \frac{3}{2}x_3^2 = -\beta \sin\theta(\sin\theta - \sqrt{3}\cos\theta) < 0,$$

because $\beta < 0$ and $\theta \in (0, \frac{1}{3}\pi)$. This, in addition with the fact that p_3 is a symmetric singularity, ensures that it is a center (see [37, Section 2]).

We now work statement (c). Observe that

$$\frac{1}{2}\beta + \frac{3}{2}x_1^2 = \frac{9}{2}\sqrt[3]{\frac{\alpha^2}{4}} > 0, \quad \frac{1}{2}\beta + \frac{3}{2}x_2^2 = 0,$$

because $\beta = -3\sqrt[3]{\frac{\alpha^2}{4}}$. Therefore, $(x_1, 0)$ is a hyperbolic saddle and $(x_2, 0)$ is degenerated. Translating $(x_2, 0)$ to the origin and then doing a quasihomogenous blow up with weight $(2, 3)$ we obtain Figure 7.

Finally, assuming the hypothesis of statement (d) we obtain $\alpha = \beta = 0$ and then the origin is the unique finite singularity and it is clearly a non-hyperbolic saddle. \square

We now study the phase portraits of X_{21} .

Proposition 8. *The phase portrait of X_{21} with $b = 1$ is the one given in Figure 20.*

Proof. First we observe that X_{21} cannot have any limit cycle because every finite singularity is symmetric. Using the same approach as in Section 2 one can conclude the phase portraits of X_{21} when $D \geq 0$. Knowing that X_{21} is also φ -reversible with $\varphi(x, y) = (-x, y)$ when $\alpha = 0$ one can conclude its phase portrait when $D < 0$ and $\alpha = 0$. Knowing that singularity $p_2 = p_3$ is a *cuspidal S-singularity* of X_{21} when $D = 0$ and $\alpha \neq 0$ one can also conclude the phase portrait for $D < 0$, but near the boundary $D = 0$. Now we must prove that this last phase portrait holds for any (α, β) such that $D < 0$ and $\alpha \neq 0$.

If $D < 0$ we know that we have three finite singularities, a center p_3 in the middle and a hyperbolic saddle p_2 on its left side and another hyperbolic saddle p_1 on its right side. Let $\mu_0 = (\alpha_0, \beta_0) \in \mathbb{R}^2$ be such that there is a heteroclinic orbit Γ_0 connecting both hyperbolic saddles, $x_0 \in \mathbb{R}^2$ the intersection of Γ_0 with the y -axis and l_0 a transversal section of Γ_0 passing through x_0 . Following [32] we define n to be the coordinate along the normal line l_0 such that $n > 0$ outside the polycycle (observe that there is another heteroclinic connection due to the symmetry) and $n < 0$ inside the polycycle. We also denote Γ_s and Γ_u the perturbations of Γ_0 , for $|(\alpha - \alpha_0, \beta - \beta_0)|$ small enough, such that Γ_s is contained in the stable manifold of p_1 and Γ_u is contained in the unstable manifold of p_2 . Let x_s and x_u be the intersections of Γ_s and Γ_u with l_0 , respectively, and let n_s and n_u be its coordinates

along the line l_0 . We now define the displacement map $d(\alpha, \beta) = n_u - n_s$. See Figure 8.

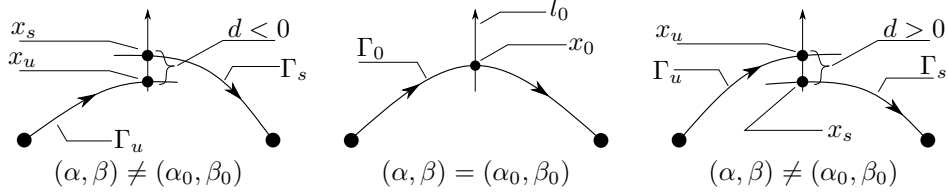


FIGURE 8. The displacement map $d(\alpha, \beta)$ defined near (α_0, β_0) .

Let $\gamma(t)$ be a parametrization of Γ_0 with $\gamma(0) = x_0$ and $f(t; \alpha, \beta) = X_{21}(\gamma(t); \alpha, \beta)$. It follows from [32] that

$$\frac{\partial d}{\partial \alpha}(\mu_0) = \frac{1}{|f(0; \mu_0)|} \int_{-\infty}^{+\infty} \left(e^{-\int_0^t \text{Div}(f(s; \mu_0)) ds} \right) f(t; \mu_0) \wedge \frac{\partial f}{\partial \alpha}(t; \mu_0) dt,$$

where $\mu_0 = (\alpha_0, \beta_0)$ and $(x_1, x_2) \wedge (y_1, y_2) = x_1 y_2 - x_2 y_1$. Knowing that

$$X_{21}(x, y; \alpha, \beta) \wedge \frac{\partial X_{21}}{\partial \alpha}(x, y; \alpha, \beta) = \frac{1}{2}y,$$

one can see that $\frac{\partial d}{\partial \alpha}(\mu_0) > 0$ whenever d is defined. Hence, given $\beta = \beta_0 < 0$ fixed and $\alpha_0 = \alpha_0(\beta_0)$ such that $d(\alpha_0, \beta_0) = 0$ we conclude that $d(\cdot, \beta_0)$ increases for $\alpha \approx \alpha_0$ and thus if α_0 exists it is unique. But we already know that $d(0, \beta) = 0$ for every $\beta < 0$ and therefore given $\beta = \beta_0 < 0$ fixed it follows that $\alpha = 0$ is the unique value that satisfy $d(\alpha_0, \beta_0) = 0$. \square

In a similar way one can prove that the phase portrait of X_{21} with $b = -1$ is the one given by Figure 21.

4. SYSTEM X_{22}

We remember that system X_{22a} is given by

$$\dot{x} = (\beta + a)xy + (\beta - a)y^3, \quad \dot{y} = \frac{\alpha}{2} + \frac{1}{2}x^2 + xy^2 + \frac{1}{2}y^4,$$

with $a \in \{-1, 1\}$. On the other hand, system X_{22b} is given by

$$\dot{x} = (\beta + 1)xy + (\beta - 1)y^3, \quad \dot{y} = \frac{\alpha}{2} + \frac{a}{2}x^2 + axy^2 + \frac{a}{2}y^4,$$

with $a \in \{-1, 1\}$. Observe that they are both equal if we replace $a = 1$. Moreover, if we replace $a = -1$ on X_{22b} and then apply the change of variables and parameters

$$(x, y; \alpha, \beta) \mapsto (x_1, -y_1; -\alpha_1, -\beta_1)$$

we obtain system X_{22a} with $a = -1$. Hence, both systems are equivalent and we focus on X_{22a} .

Let $S_x = \{(x, y) \in \mathbb{R}^2 : \dot{x}(x, y) = 0\}$ and $S_y = \{(x, y) \in \mathbb{R}^2 : \dot{y}(x, y) = 0\}$ and observe that

$$S_x = \{(x, y) \in \mathbb{R}^2 : y = 0 \text{ or } x = \frac{a-\beta}{a+\beta}y^2\},$$

$$S_y = \{(x, y) \in \mathbb{R}^2 : x = -y^2 \pm \sqrt{-\alpha}\}.$$

Proposition 9. *The phase portrait of X_{22a} with $a = 1$ is given by Figure 22.*

Proof. Here we point out only some particular reasonings. Approaching system X_{22a} as in Section 2 and knowing that the *Bendixson Criterion* prevents the existence of any limit cycles in this case, one can work with the separatrices. But here one must look also at the flows at sets S_x and S_y . Take for example Figure 9. One can obtain it with an analysis of the flow on the sets S_x and S_y together with

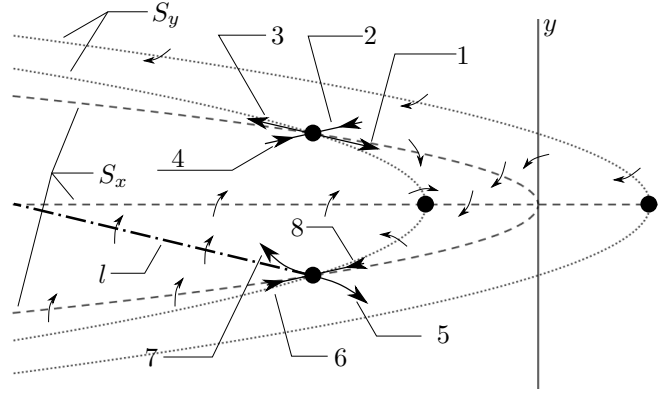


FIGURE 9. Illustration of the flow of X_{22a} with $a = 1$ and $\beta < -1$ at the sets S_x and S_y .

an analysis at the eigenvectors of the hyperbolic saddles. Now one can conclude that separatrix 1 must cross the x -axis and thus it must glue with separatrix 8 due to symmetry. At other hand, separatrix 3 is trapped between the x -axis and S_y and thus it must end at infinity. Finally, separatrix 7 has no other option than either ending at infinity (precisely at the west pole) or crossing the x -axis. Let $q = q(\alpha, \beta)$ be the hyperbolic saddle inside the half-plane $y < 0$ and $\lambda^- < 0 < \lambda^+$, $\lambda^\pm = \lambda^\pm(\alpha, \beta)$, the eigenvalues of $DX_{22a}(q)$. Let $v = v(\alpha, \beta)$ be an eigenvector of $DX_{22a}(q)$ with respect to λ^+ , $l(t) = q + tv$ and $t_0 = t_0(\alpha, \beta)$ such that $l(t_0)$ is the intersection of l and the x -axis. Calculations shows that separatrix 7 is above l and if t is between 0 and t_0 , then the flow of X_{22a} is transversal to l and it points upwards. Therefore separatrix 7 cannot cross l and thus it must cross the x -axis and hence it glues up with separatrix 4 due to the symmetry.

The local phase portrait of X_{22a} with $a = 1$, $\beta = -1$ and $\alpha \leq -16$ is shown in Figure 10. To prove that separatrix 2, which born at the singularity $p = (\sqrt{-\alpha}, 0)$, ends at the north pole we calculate the flow on the parabola $x = -\frac{1}{2}y^2 + \sqrt{-\alpha}$ and observe that it points upwards if $y \neq 0$. We also calculate that separatrix 2 near p is given by $(f(y), y)$, where

$$f(y) = -\frac{\sqrt{-4\sqrt{-\alpha} - \alpha} + \alpha}{2\alpha}y^2 + O(y^4).$$

Knowing that

$$-\frac{1}{2} \leq -\frac{\sqrt{-4\sqrt{-\alpha} - \alpha} + \alpha}{2\alpha},$$

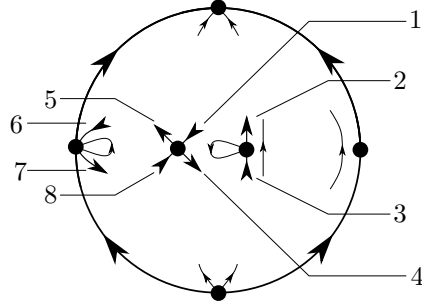


FIGURE 10. Local phase portrait of X_{22a} with $a = 1$, $\beta - 1$ and $\alpha \leq -16$.

with the right hand side equals $-\frac{1}{2}$ if and only if $\alpha = -16$, one can conclude that if $\alpha < -16$, then separatrix 2 ends at the north pole. Moreover, if $\alpha = -16$, then

$$f(y) = -\frac{1}{2}y^2 + \frac{1}{32}y^4 + O(y^6),$$

and thus separatrix 2 goes to the north pole in this case too. \square

Proposition 10. *The phase portrait of X_{22a} with $a = -1$ is the one given by Figure 23.*

Proof. Here we point out two things. First we assume $\alpha < 0$ and $\beta \geq 1 + 2\sqrt{-\alpha}$. In this case one can see that the local phase portrait is given by Figure 11. We

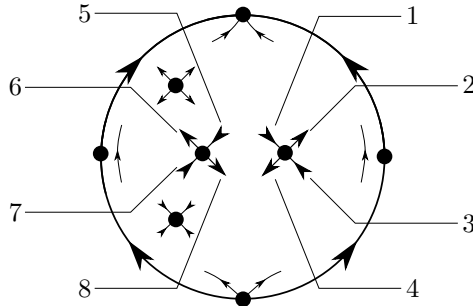
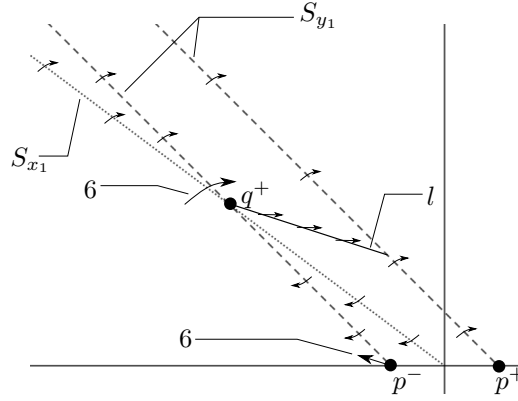


FIGURE 11. Local behavior of the phase portrait of X_{22a} with $a = -1$, $\alpha < 0$ and $\beta \geq 1 + 2\sqrt{-\alpha}$.

want to prove that for β big enough separatrix 6 must end at the north pole. Doing the change of coordinates $(x, y) = (x_1, \sqrt{y_1})$ for $y > 0$ one get the vector field $X_1 = X_1(x_1, y_1)$ whose differential system is

$$\dot{x}_1 = \sqrt{y_1}((\beta - 1)x_1 + (\beta + 1)y_1), \quad \dot{y}_1 = \sqrt{y_1}(\alpha + x_1^2 + 2x_1y_1 + y_1^2).$$

The fact that separatrix 6 at system X_{22a} crosses the set S_x above the unstable node implies, for the system X_1 , that separatrix 6 also crosses the set S_{x_1} above the unstable node q^+ . See Figure 12. Taking $\beta \geq 1 + 2\sqrt{-\alpha} + 4\sqrt[4]{-\alpha}$ and defining


 FIGURE 12. Illustration of the flow of X_1 at the sets S_{x_1} and S_{y_1}

the line

$$l = q^+ + t \left(1, \frac{\alpha}{(-\alpha)^{\frac{3}{4}} - \alpha} \right)$$

one can conclude that the flow crosses l upwards and thus separatrix 6 must cross the line of S_{y_1} which contains p^+ . But at the right hand side of this line we have $\dot{y}_1 > 0$ and thus separatrix 6 cannot end at p^+ and hence it must end at the north pole.

Second, we must prove that the relative position of the curves $\beta_1(\alpha)$ and $\beta_h(\alpha) = 1 + 2\sqrt{-\alpha}$ is as it is shown in Figure 23, i.e. we must prove $\beta_1 < \beta_h$ for $\alpha < 0$ large enough and $\beta_h < \beta_1$ for $\alpha < 0$ small enough. We remember that β_1 represents the moment when it exists a heteroclinic connection between both saddles. From now on we assume $(\alpha, \beta) = (\lambda, 1 + 2\sqrt{-\lambda})$, $\lambda \leq 0$, and we prove that for $\alpha < 0$ large enough the connection already broke and thus $\beta_1 < \beta_h$. Translating the saddle to the left of the origin and then doing a simple blow up in the y direction one obtain the vector field $X_2 = X_2(x_2, y_2)$ whose differential system is

$$\dot{x}_2 = 2\lambda + \sqrt{-\lambda}x_2^2 + 3\sqrt{-\lambda}x_2y_2 + 2(1 + \sqrt{-\lambda})y_2^2 - \frac{1}{2}x_2^3y_2 - x_2^2y_2^2 - \frac{1}{2}x_2y_2^3,$$

$$\dot{y}_2 = -\sqrt{-\lambda}x_2y_2 - \sqrt{-\lambda}y_2^2 + \frac{1}{2}x_2^2y_2^2 + x_2y_2^3 + \frac{1}{2}y_2^4.$$

In these coordinates set S_{x_2} has a closed component. Let $p_1 = (x_0, y_0)$ be the higher point in this closed component. Calculations shows that p_1 lies on the left of the straight line r given by $x_2 + y_2 = -\sqrt{-\lambda}$. Let $p_2 = (-y_0, y_0)$ be the projection of p_1 on r and observe that p_2 is above the focus p_3 , which lies in the same line. See Figure 13. It follows from an analysis on the set S_{x_2} that the separatrix s must cross r above the point p_2 . Let l be the segment given by $p_2 + t(1, -\frac{1}{2})$ such that it ends at the other component r_1 of S_{y_2} . For $\alpha < 0$ large enough calculations shows that the flow on l points upwards and thus separatrix s must cross r_1 . But at the right side of r_1 we have $\dot{y}_1 > 0$ and thus s must end at the north pole. Therefore, for $\alpha < 0$ large enough we have $\beta_1 < \beta_h$. Once we cannot give β_1 explicitly and that there is nothing that prevents either $\beta_1 < \beta_h$ or $\beta_h < \beta_1$ it turns out to be a very difficult task to understand completely and in a analytic way the relative position of β_h and β_1 . But numerical computations (see chapters 9 and 10 of [17]) shows that for $\lambda_0 \approx -\frac{2}{3}$ is the unique intersection of β_1 and β_h . Moreover it also

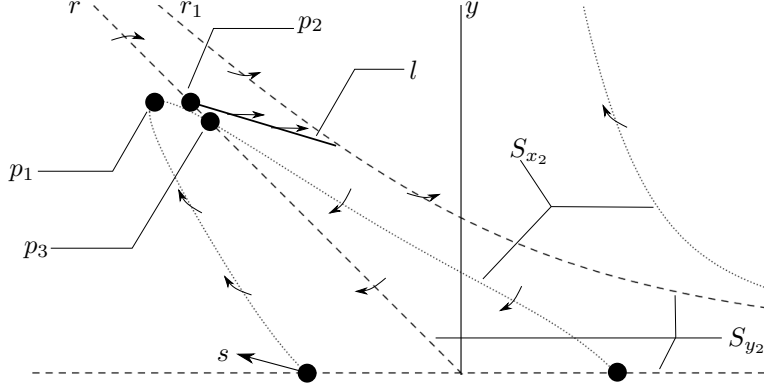


FIGURE 13. Illustration of the flow of X_2 at the sets S_{x_2} and S_{y_2} .

shows that $\beta_h < \beta_1$ if $\lambda \in (\lambda_0, 0)$ and $\beta_1 < \beta_h$ if $\lambda \in (-\infty, \lambda_0)$. So to provide an analytic proof of these facts is an open problem. \square

5. SYSTEM X_{23}

Let us remember that system X_{23} is given by

$$\dot{x} = a\alpha xy - y^3 + ax^3y + axy^5, \quad \dot{y} = \frac{\beta}{2} + \frac{a}{2}x - \frac{\alpha}{2}y^2 - \frac{1}{2}x^2y^2 - \frac{1}{2}y^6,$$

with $a \in \{-1, 1\}$.

Since this system has a particular higher degree than the previous systems it is not practical to find analytic expressions for the finite singularities as we did with the previous systems. Therefore, we change our approach. First we do the change of variables given by $(x, y) = (x_1, \sqrt{y_1})$, obtaining the vector field

$$\dot{x}_1 = \sqrt{y_1}(-y_1 + x_1(x_1^2 + y_1^2 + \alpha)), \quad \dot{y}_1 = \sqrt{y_1}(x_1 - y_1(x_1^2 + y_1^2 + \alpha) + \beta).$$

Dividing both equations by $\sqrt{y_1}$ we obtain the vector field $Y = (\dot{x}_2, \dot{y}_2)$ given by

$$(3) \quad \dot{x}_2 = -y_2 + x_2(x_2^2 + y_2^2 + \alpha), \quad \dot{y}_2 = x_2 - y_2(x_2^2 + y_2^2 + \alpha) + \beta.$$

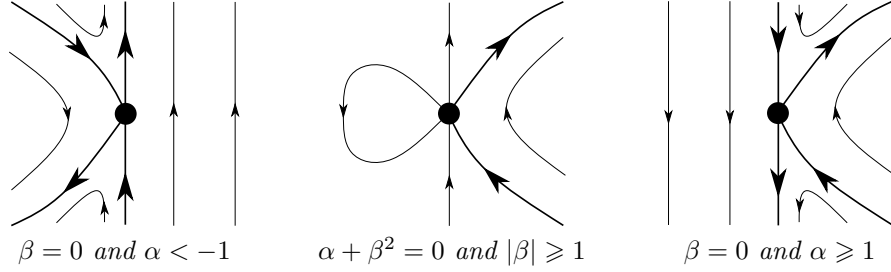
Observe that X_{23} and Y are topologically equivalent for $y > 0$ (which is equivalent to $y_2 > 0$) and Y has degree 3 while X_{23} has degree 6. Therefore, the approach is the following. We study the vector field Y at $y_2 > 0$ and then draw conclusions for X_{23} for $y > 0$ (and thus for $y < 0$ too due to its symmetry) and study locally the unique singularity $p = (-a\beta, 0)$ of X_{23} at the x -axis. From now on we focus on the case $a = 1$.

Proposition 11. *The following statement hold.*

- (a) p is a hyperbolic saddle if $\beta(\alpha + \beta^2) < 0$ and a center if $\beta(\alpha + \beta^2) > 0$.
- (b) p is a center if $\{\beta = 0, -1 \leq \alpha < 1\}$ or $\{\alpha + \beta^2 = 0, |\beta| < 1\}$.
- (c) Otherwise the local phase portrait of X_{23} at p is given in Figure 14.

Proof. Statement (a) follows from

$$DX_{23}(p) = \begin{pmatrix} 0 & -\beta(\alpha + \beta^2) \\ \frac{1}{2} & 0 \end{pmatrix},$$


 FIGURE 14. Local phase portraits of X_{23} at p .

and the fact that p is a symmetric singularity. Statements (b) and (c) follow from a quasihomogeneous blow up with weight (2, 1). \square

Let us define the following functions.

$$\begin{aligned}
 p_1(x_2) &= 2x_2^2 + \beta x_2 + \alpha. \\
 p_2(x_2) &= 4x_2^5 + 5\beta x_2^4 + (4\alpha + \beta^2)x_2^3 + 2\alpha\beta x_2^2 + (\alpha^2 - 1)x_2 - \beta; \\
 (4) \quad f(x_2) &= \sqrt{x_2(x_2 + \beta)}. \\
 R(\alpha, \beta) &= -256(\alpha^2 - 1)^3 - 192\alpha(\alpha^4 + 7\alpha^2 + 28)\beta^2 \\
 &\quad + 60(\alpha^4 - 28\alpha^2 - 72)\beta^4 - 4\alpha(\alpha^2 - 108)\beta^6 - 27\beta^8.
 \end{aligned}$$

In what follows we list some analytic properties of the finite singularities of Y when $y_2 > 0$.

Proposition 12. *Let $q = (x_0, y_0) \in \mathbb{R}^2$ such that $y_0 > 0$. The following statements hold.*

(a) q is a finite singularity of Y if, and only if,

$$y_0 = \frac{x_0 + \beta}{p_1(x_0)} = x_0 p_1(x_0) = f(x_0).$$

(b) If q is a finite singularity of Y , then $p_2(x_0) = 0$ and $x_0 p_1(x_0) > 0$.

(c) If $q_0 = (x_0, f(x_0))$ is such that $p_2(x_0) = 0$ and $x_0 p_1(x_0) > 0$, then q_0 is a finite singularity of Y .

(d) If q is a non-hyperbolic finite singularity of Y , then $\beta = 0$ or $R(\alpha, \beta) = 0$.

Proof. Isolating $u = x_2^2 + y_2^2 + \alpha$ from $\dot{x}_2 = 0$ and $\dot{y}_2 = 0$ we see that a necessary condition for a point (x_0, y_0) be a singularity of Y is that it satisfies

$$\frac{y_0}{x_0} = \frac{x_0 + \beta}{y_0}.$$

Knowing that $y_0 > 0$ we obtain $y_0 = f(x_0)$. Statement (a) now follows from $Y(x_0, f(x_0)) = (0, 0)$.

From statement (a) one concludes that if q is a finite singularity of Y , then $x_0 p_1^2(x_0) - (x_0 + \beta) = 0$ and $x_0 p_1(x_0) = f(x_0) \geq 0$. Statement (b) now follows from the fact that $x_0 \neq 0$ and $p_2(x_0) = x_0 p_1^2(x_0) - (x_0 + \beta)$.

To prove statement (c) first observe that $p_2(x_0) = 0$ implies $x_0 p_1(x_0)^2 = x_0 + \beta$ and thus

$$x_0 p_1(x_0)^2 = x_0 + \beta = \frac{f(x_0)^2}{x_0}.$$

Hence, $x_0^2 p_1(x_0)^2 = f(x_0)^2$. Squaring both sides and knowing that $x_0 p_1(x_0) > 0$ we obtain statement (c).

Now observe that the Jacobian matrix of Y is given by

$$DY(x_2, y_2) = \begin{pmatrix} 3x_2^2 + y_2^2 + \alpha & 2x_2 y_2 - 1 \\ 1 - 2x_2 y_2 & -(x_2^2 + 3y_2^2 + \alpha) \end{pmatrix}.$$

Replacing $y_0 = f(x_0)$ and calculating the trace and the determinant and then replacing $f(x_0) = x_0 p_1(x_0)$ we obtain

$$(5) \quad \text{Tr}(x_0) = -2x_0\beta, \quad \text{Det}(x_0) = -p_2'(x_0).$$

It follows from the *Trace-Determinant Characterization* (see Section 4.1 of [21]) that a singularity q is non-hyperbolic if $\text{Tr}(x_0) = 0$, $\text{Det}(x_0) = 0$ or both. Therefore, if $q = (x_0, y_0)$, $y_0 > 0$, is a singularity, then it follows from (3) that $x_0 \neq 0$ and thus $\text{Tr}(x_0) = 0$ if, and only if, $\beta = 0$. Moreover, since $R(\alpha, \beta)$ is the *resultant* (except by a constant) with respect to the variable x_2 between p_2 and p_2' it follows from (5) and from statement (b) that $\text{Det}(x_0) = 0$ if, and only if, $R(\alpha, \beta) = 0$. \square

In what follows we list some properties of $R(\alpha, \beta)$ (see (4)) and the parabola $\alpha + \beta^2 = 0$.

Proposition 13. *The following statement holds.*

- (a) $R(\alpha, \beta) = 0$ has four branches (two positives and two negatives) if $\alpha \leq -1$, two branches (one positive and one negative) if $-1 < \alpha \leq 1$ and no branches at all if $\alpha > 1$.
- (b) Let β_+ be the negative branch that borns at $\alpha = 1$ and β_- the negative branch that borns at $\alpha = -1$. Then $\mu_1 \approx (-3.398\dots, -1.849\dots)$ is the unique intersection between β_+ and β_- .
- (c) $\mu_2 \approx (-3.389\dots, -1.841\dots)$ is the unique intersection between the parabola $\alpha + \beta^2 = 0$ and $R(\alpha, \beta) = 0$ at $\beta < 0$. Moreover it occurs at β_- . See Figure 15.

Proof. Fortunately $R(\alpha, \beta)$ is biquadratic at β and thus we can do the change of variables $\beta \mapsto \pm\sqrt{b}$ (both give the same result) and obtain the quartic polynomial in b

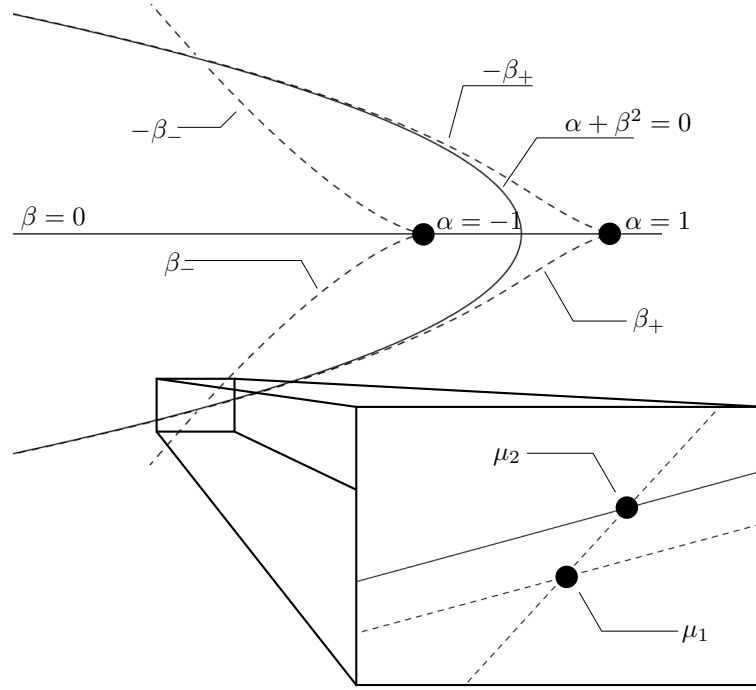
$$\begin{aligned} R_1(\alpha, b) = & -256(\alpha^2 - 1)^3 - 192\alpha(\alpha^4 + 7\alpha^2 + 28)b \\ & + 60(\alpha^4 - 28\alpha^2 - 72)b^2 - 4\alpha(\alpha^2 - 108)b^3 - 27b^4. \end{aligned}$$

Given $\alpha_0 \in \mathbb{R}$ fixed we want to know how many positive real roots the polynomial $R_1(\alpha_0, b)$ has. We recall that if

$$P(x) = a_4 x^4 + a_3 x^3 + a_2 x^2 + a_1 x + a_0$$

is a real polynomial of degree four and r_1, r_2, r_3 and r_4 are its roots, then its discriminant (see [16] p. 157) is given by

$$a_4^6 \prod_{i < j} (r_i - r_j)^2.$$


 FIGURE 15. Plot of the sets $R(\alpha, \beta) = 0$ and $\alpha + \beta^2 = 0$.

The discriminant in b of R_1 is given (see chapter 12 of [16] for an expression of the discriminant in function of the coefficients), except by a constant, by

$$\begin{aligned}
 D(\alpha) = & -1\,871\,773\,696 - 10\,034\,479\,104\,\alpha^2 - 19\,980\,402\,688\,\alpha^4 \\
 & - 17\,398\,321\,152\,\alpha^6 - 5\,393\,464\,832\,\alpha^8 + 250\,599\,680\,\alpha^{10} \\
 & + 64\,492\,352\,\alpha^{12} + 870\,480\,\alpha^{14} - 190\,633\,\alpha^{16} - 9\,567\,\alpha^{18} \\
 & - 167\,\alpha^{20} - \alpha^{22}.
 \end{aligned}$$

Computations show that $D(\alpha) \leq 0$ with the equality happening only if $\alpha = \pm 3.398\dots$. It is well known (see [16] p. 45) that if $D < 0$, then R_1 has two distinct real roots and two complex conjugate roots. If $\{b_1, b_2, b_3, b_4\}$ are the four roots in b of R_1 , then

$$R_1(\alpha, \beta) = -27(b - b_1)(b - b_2)(b - b_3)(b - b_4)$$

and thus $27b_1b_2b_3b_4 = 256(\alpha^2 - 1)^3$. Supposing that b_1, b_2 are the real solutions and b_3, b_4 the complex solutions we conclude that $\text{sign}(b_1b_2) = \text{sign}(\alpha^2 - 1)$. Hence, there is a unique positive solution when $-1 < \alpha < 1$. Moreover b_1 and b_2 can change sign only if $\alpha = \pm 1$. Choosing arbitrarily $\alpha = \pm 2$ we see that there is no positive solution for $\alpha = 2$ and there are two positive real solutions for $\alpha = -2$. Hence we conclude that there is no branch of positive solutions of R_1 if $\alpha > 1$; one branch if $-1 < \alpha \leq 1$ and two branches if $\alpha \leq -1$. Squaring those branches and then reflecting them at the x -axis one can conclude statement (a). For more details about the nature of the roots of a polynomial of degree four see [34].

If the two branches β_{\pm} intersect each other, then we have a double positive real solution of R_1 which requires $D(\alpha) = 0$ and thus $\alpha = -3.398\dots$ Replacing this at R_1 one can see that there is two complex conjugate solutions and a double positive real root and thus we have statement (b).

Knowing that $R(\alpha, -\sqrt{-\alpha}) = 256 + 288\alpha^2 - 27\alpha^4$ one can calculate its roots and see that the unique root $\alpha_0 \leq -1$ is given by $\alpha_0 = -\frac{4}{3}\sqrt{3 + 2\sqrt{3}}$ and thus $\mu_2 = (\alpha_0, -\sqrt{-\alpha_0})$ is the unique intersection between the sets $\alpha + \beta^2 = 0$ and $R(\alpha, \beta) = 0$. The relative position of μ_1, μ_2 and the parabola $\alpha + \beta^2 = 0$ and the fact that β_{\pm} are the graphs of some continuous function implies that $\mu_2 \in \beta_-$ and thus we have statement (c). \square

Numerical computations show that the branches $-\beta_{\pm}$ of $R(\alpha, \beta) = 0$ perturb the double roots x_0 of p_2 which do not satisfy $x_0 p_1(x_0) > 0$ and thus perturb the roots that are not related to the finite singularities of Y and thus can be ignored. Moreover, the negative branches β_{\pm} perturb the double roots x_0 of p_2 which do satisfy $x_0 p_1(x_0) > 0$ and thus perturb the roots that are related to the finite singularities. One can now draw the backbone of the bifurcation diagram of X_{23} , with $a = 1$, and thus obtain the solid lines of Figure 31.

Proposition 14. *Let $(\alpha_0, \beta_0) \in \mathbb{R}^2$ such that $\beta_0 = \beta_{\pm}(\alpha_0)$ (i.e. it is a point in one of the branches β_{\pm}), with $\beta_0 < 0$, and $\gamma(t) = (t + \alpha_0, \beta_0)$, $|t| < \varepsilon$, a transversal segment through β_{\pm} . Then a saddle-node bifurcation happens at $\gamma(0)$ in such way that it vanishes when t increases.*

Proof. We know that at $t = 0$ we have a double real root x_0 of p_2 which satisfy $x_0 p_1(x_0) > 0$. Therefore, it follows from statement (c) of Proposition 12 that $q_0 = (x_0, f(x_0))$ is a non-hyperbolic finite singularity of X_{23} . Since $\beta_0 < 0$ we know that the trace of $DX_{23}(q_0)$ is not zero and thus $DX_{23}(q_0)$ has only one eigenvalue equal zero. Hence, q_0 is a non-hyperbolic saddle, a non-hyperbolic node or a saddle-node.

Computations show that if $t < 0$, then the double root x_0 splits in two simple real roots x_-, x_+ satisfying $x_{\pm} p_1(x_{\pm}) > 0$. Hence, it follows from Proposition 12 that $q_{\pm} = (x_{\pm}, f(x_{\pm}))$ are both hyperbolic finite singularities of X_{23} . The proof now follows from the fact that if $t > 0$, then the double real root x_0 goes to the complex realm and thus the finite singularity q_0 vanishes. \square

Calculating the infinity of X_{23} , with $a = 1$, one can see that the only singularities are the origins of the charts U_1 and U_2 . While the origin of U_2 is an unstable node the local phase portrait at the origin of U_1 is given by Figure 16. To prove this

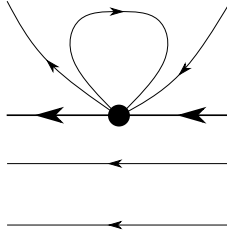


FIGURE 16. Local phase portrait of $p(X_{23})$, with $a = 1$, at the origin of U_1 .

last claim one must do a quasihomogeneous directional blow up at the direction x^+ with weight (3, 2) and then a quasihomogenous blow up with $(\alpha, \beta) = (1, 4)$ at the unique singularity that appear. Hence it follows from Theorem 3 that *the sum of the Poincaré indices of all the finite singularities must always be equal to -1 .*

It follows from the characterization given at Definition 4 that X_{23} with $a = 1$ is topologically equivalent at $p = (-\lambda, 0)$ to the origin of:

- (a) X_{12} when $\alpha_0 + \beta_0^2 = 0$, $|\beta_0| \geq 1$ and $|\beta - \beta_0| < \varepsilon$.
- (b) X_{13} when $\beta_0 = 0$, $|\alpha_0| > 1$ and $|\beta| < \varepsilon$.
- (c) X_{14} when $\alpha_0 + \beta_0^2 = 0$, $0 < |\beta_0| < 1$ and $|\beta - \beta_0| < \varepsilon$.

Although we have the local equivalence between p at X_{23} and the origin of X_{12} , X_{13} or X_{14} we do not have the direction of the bifurcation, i.e. as β increases do λ increase or decrease? The following proposition solves this question.

Proposition 15. *Let λ be the parameter of X_{12} , X_{13} and X_{14} and $(\alpha_0, \beta_0) \in \mathbb{R}^2$ fixed. The following statement holds.*

- (a) *If $\alpha_0 + \beta_0^2 = 0$, $|\beta_0| \geq 1$ and $|\beta - \beta_0| < \varepsilon$, then as $|\beta|$ increases λ also increases.*
- (b) *If $\beta_0 = 0$, $|\alpha_0| > 1$ and $|\beta| < \varepsilon$, then as β increases λ increases if $\alpha_0 > 1$ and decreases if $\alpha_0 < -1$.*
- (c) *If $\alpha_0 + \beta_0^2 = 0$, $0 < |\beta_0| < 1$ and $|\beta - \beta_0| < \varepsilon$, then as β increases λ also increases.*

Proof. All statements follow from statement (a) of Proposition 11 and the fact that if $\lambda > 0$, then X_{12} , X_{13} and X_{14} has a lonely center while if $\lambda < 0$ it have a hyperbolic saddle. \square

Finally we point out that at $\beta = 0$ and $\alpha < -1$ we have a center-focus problem at the singularity $p_0 = \frac{1}{\sqrt{2}}(-\sqrt{-1-\alpha}, \sqrt{-1-\alpha})$ of Y . Translating this singularity to the origin one obtain the vector field Y_1 whose differential system is

$$\begin{aligned} \dot{x} &= -(2 + \alpha)x + \alpha y - \frac{3}{\sqrt{2}}\sqrt{-1-\alpha}x^2 + \sqrt{2}\sqrt{-1-\alpha}xy - \frac{\sqrt{-1-\alpha}}{\sqrt{2}}y^2 \\ &\quad + x^3 + xy^2 \\ \dot{y} &= -\alpha x + (2 + \alpha)y - \frac{\sqrt{-1-\alpha}}{\sqrt{2}}x^2 + \sqrt{2}\sqrt{-1-\alpha}xy - \frac{3}{\sqrt{2}}\sqrt{-1-\alpha}y^2 \\ &\quad - x^2y - y^3. \end{aligned}$$

Knowing that the vector field Y_1 is φ -reversible with $\varphi(x, y) = (-y, -x)$ we conclude that p_0 is a center.

Proposition 16. *The phase portraits of X_{23} with $a = 1$ are the one given in Figures 31, 32, 33 and 34.*

Proof. With an analysis of $f(x_2)$ and $x_2p_1(x_2)$ (see the functions defined at (4)) one can see that in region 1 of Figure 31 there is only one pair of singularities aside $p = (-\lambda, 0)$ and in region 23 there is no other singularity other than p .

Using the same techniques as in the previous systems, and the information that we already have, one can obtain the phase portraits 1, 2, 3, 4, 5, 13, 23, 31 and 32. Looking at 13 and 23 and knowing that at 22 we have the collapse of a node and a saddle in a saddle-node one can obtain 22. Again if we collapse the saddle and

the node in 5 in a saddle-node we obtain the phase portrait 14. As we get down at β_- this saddle-node get away from p and phase portraits 15 and 16 rise and with them 6 and 7, respectively.

At the intersection of β_+ and the $\beta = 0$ if get down at β_+ , then a saddle-node born at p . Calculations shows that near $\beta = 0$ the direction of the unstable manifold of this saddle-node is very near the direction of the straight line $y = x$ and thus we obtain 24. As we follow β_+ the direction of the unstable manifolds approach the direction of $y = 0$ and then we can get 25 and 26. Looking at 26 and 22 we can have 21. If we split the right hand saddle-node of 21 in a saddle and a node we obtain 20. Again if we split the left hand saddle-node of 20 we obtain 11. From 20 and 32 and knowing the bifurcation that happens at p at $\alpha + \beta^2 = 0$ we can obtain 19. Now we can get 17 and 18 if we look at 16 and 19. From them one can obtain 8, 9 and 10. From 11 and 13 we have 12. From 24 we obtain 27. From 26 we obtain 29. From 27 and 29 we obtain 28. From 29 and 31 we obtain 30.

We observe that it follows from the continuity that it is impossible that the curves defined by 8 and 6 intercept each other. On the other hand we do not know if the curves defined by 28 and 30 intercept each other. But combining the bifurcation of 28 and 30 we know that if the curves intercept each other, then we have the phase portrait of Figure 34, and thus region defined by 29 is disconnected. \square

Let $X_{23a} = (P, Q)$ be X_{23} with $a = 1$ and X_{23b} be X_{23} with $a = -1$. Observe that if we do the change of coordinates $(x, y) \mapsto (-x, y)$ at X_{23a} , then we obtain $X_{23b} = (-P, Q)$. Hence a huge amount of information of X_{23a} can be carry on to X_{23b} . The most important ones are the following.

1. The relative position of the finite singularities are the same. Hence, the solid lines of Figure 31 are carried onto the bifurcation diagram of X_{23b} .
2. The determinant of the Jacobian matrices at the finite singularities are the same except by a factor of -1 . Therefore, if q is a saddle (focus/node) of X_{23a} , then it is a focus/node (saddle) of X_{23b} .
3. If $\beta(\alpha + \beta^2) \neq 0$, then $p = (-\beta, 0)$ is center (saddle) at X_{23a} if, and only if, it is a saddle (center) at X_{23b} .

With the same approach as the previous cases, mainly X_{23a} , one can conclude the following proposition.

Proposition 17. *The phase portraits of X_{23} with $a = -1$ are the ones given in Figures 35 and 36.*

6. SYSTEMS X_{24} AND X_{25}

Let us remember that X_{24} is given by

$$\dot{x} = axy + \alpha y^3, \quad \dot{y} = \frac{\beta}{2} + \frac{1}{2}x + \frac{a}{2}y^2,$$

where $a \in \{-1, 1\}$. First we observe that if we replace $a = -1$ and then do the change of variables

$$(x, y, \alpha, \beta) = (-x_1, -y_1, \alpha_1, -\beta_1),$$

then we get the same system with $a = 1$. Therefore from now on we assume $a = 1$. In this system we point out that it is the unique system which the maximum degree depends on the parameters. Observe that the maximum degree is three if $\alpha \neq 0$ and two if $\alpha = 0$. Therefore, one must do an analysis at each case. Here we only

point out some information about the local phase portrait at the origin of chart U_1 for $\alpha = 1$ and $\beta \neq 0$. In this case the local phase portrait of the blow up is incomplete due to the existence of two singularities with a unique eigenvalue (the radial one) equal zero. See Figure 17. Calculations show that in this case a center

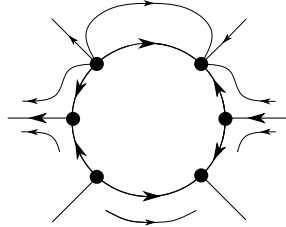


FIGURE 17. Unfinished blow up of the origin of chart U_1 of X_{24} with $\alpha = 1$.

manifold of the origin of the chart U_1 such that $v < 0$, $|v| < \varepsilon$, is given by the graph of

$$v(u) = -u^2 - \frac{\beta}{2}u^4 + O(u^6).$$

This in addition with the fact that

$$\dot{v}|_{\alpha=1} = -uv(u^2 + v),$$

it is enough to calculate the direction of the flow on the center manifold and thus to complete the blow up when $\beta \neq 0$. See Figure 18.

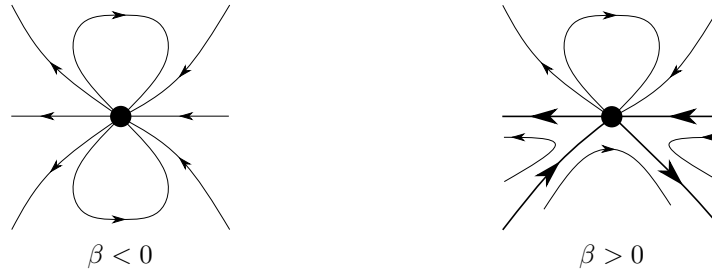


FIGURE 18. Local phase portrait of X_{24} at the origin of the chart U_1 with $a = 1$, $\alpha = 1$ and $\beta \neq 0$.

Let us remember that system X_{25b} is given by

$$\dot{x} = axy, \quad \dot{y} = \frac{\beta}{2} + \frac{\alpha}{2}x + \frac{\delta}{2}x^2 + \frac{b}{2}y^2,$$

where $ab > 0$, $\delta \in \{-3, 3\}$ and

$$\{(a \in \{-1, 1\}, b \in \{-3, 3\}) \text{ or } (a \in \{-3, 3\}, b \in \{-1, 1\})\}.$$

Here we observe that with the change of variables

$$(x, y, \alpha, \beta) \rightarrow (x_1, -y_1, -\alpha_1, -\beta_1),$$

it is enough to study only the four cases given by

- (a) $a = 1$, $b = 3$ and $\delta = 3$.
- (b) $a = 1$, $b = 3$ and $\delta = -3$.
- (c) $a = 3$, $b = 1$ and $\delta = 3$.
- (d) $a = 3$, $b = 1$ and $\delta = -3$.

ACKNOWLEDGMENTS

This work is supported by Agencia Estatal de Investigación grant PID2022-136613NB-100, AGAUR (generalitat de Catalunya) grant 2021SGR00113 and by the Reial Acadèmia de Ciències i Arts de Barcelona, by CNPq grant 304798/2019-3, by Agence Nationale de la Recherche (ANR), project ANR-23-CE40-0028, and São Paulo Research Foundation (FAPESP), grants 2021/01799-9 and 2023/02959-5.

APPENDIX A. LOCAL LINEARIZATION OF THE INVOLUTION

Let $Q: \mathbb{R}^m \rightarrow \mathbb{R}^m$ be a linear involution, i.e. a linear map such that $Q = Q^{-1}$ (also known as *involuntary matrix*). Then the following statements hold.

- (i) If $\lambda \in \mathbb{C}$ is a eigenvalue of Q , then $\lambda \in \{-1, 1\}$.
- (ii) Q is diagonalizable.

Indeed, let $\lambda \in \mathbb{C}$ be a eigenvalue of Q and $x \in \mathbb{R}^m$, $x \neq 0$, one of its eigenvectors. Since Q^2 is the identity map it follows that,

$$x = Q^2x = Q(Qx) = \lambda Qx = \lambda^2x.$$

In particular we have that $\lambda^2 = 1$ and thus $\lambda \in \{-1, 1\}$, proving statement (i).

We now prove statement (ii). Suppose by contradiction that Q is not diagonalizable. Then its Jordan canonical form (see [33, Chapter 4.5]) has at least one Jordan block of size $k \geq 2$. Hence there is a eigenvalue $\lambda \in \mathbb{C}$ of Q and vectors $u, v \in \mathbb{R}^m \setminus \{0\}$ such that

$$Qu = \lambda u, \quad Qv = u + \lambda v.$$

Now observe that,

$$v = Q^2v = Q(u + \lambda v) = \lambda u + \lambda(u + \lambda v) = 2\lambda u + \lambda^2v.$$

From statement (i) we know that $\lambda^2 = 1$ and thus we obtain $0 = 2\lambda u$, which in turn implies $\lambda = 0$ contradicting (i).

Proposition 18. *Let $\varphi: \mathbb{R}^m \rightarrow \mathbb{R}^m$ be an involution such that $\text{Fix}(\varphi)$ is an embedded sub-manifold of dimension $r \in \{0, \dots, m\}$. If $p \in \text{Fix}(\varphi)$, then there is a neighborhood of p such that φ is C^k -conjugated to*

$$\Phi(x_1, \dots, x_m) = (x_1, \dots, x_r, -x_{r+1}, \dots, -x_m).$$

Proof. Let $T(x) = x + p$ and $\psi(x) = T^{-1} \circ \varphi \circ T$. Observe that $\psi(0) = 0$ and $\psi = \psi^{-1}$. Therefore φ is conjugate to another involution ψ such that $\psi(0) = 0$ and thus we can suppose $p = 0$. Let $Q = D\varphi(0)$ and $\sigma(x) = x + Q\varphi(x)$. Since $\varphi = \varphi^{-1}$ and $\varphi(0) = 0$ it follows that,

$$(6) \quad Q^{-1} = [D\varphi(0)]^{-1} = D\varphi^{-1}(\varphi(0)) = D\varphi(\varphi(0)) = D\varphi(0) = Q.$$

In particular we have that $D\sigma(0) = 2\text{Id}_{\mathbb{R}^m}$ and thus from the Inverse Function Theorem it follows that σ is locally a C^k -diffeomorphism at the origin. Observe that

$$\sigma(\varphi(x)) = \varphi(x) + Qx = Q(Q\varphi(x) + x) = Q\sigma(x).$$

Therefore σ conjugates φ and Q . In particular it follows that $\text{Fix}(Q) \subset \mathbb{R}^m$ is sub vector space of dimension r . From (6) we know that Q is an involution. Thus from statements (i) and (ii) we have that there is a linear change of variables such that in these new variables Q is given by,

$$Q(x_1, \dots, x_m) = (x_1, \dots, x_r, -x_{r+1}, \dots, -x_m).$$

The result now follows from the fact that φ is C^k -conjugated to Q by σ . \square

APPENDIX B. POINCARÉ COMPACTIFICATION

Let X be a planar *polynomial* vector field of degree n as our polynomial differential systems of Theorem 1. The *Poincaré compactified vector field* $p(X)$ is an analytic vector field on \mathbb{S}^2 constructed as follow (for more details see [17, Chapter 5]).

First we identify \mathbb{R}^2 with the plane $(x_1, x_2, 1)$ in \mathbb{R}^3 and define the *Poincaré sphere* as $\mathbb{S}^2 = \{y = (y_1, y_2, y_3) \in \mathbb{R}^3 : y_1^2 + y_2^2 + y_3^2 = 1\}$. We define the *northern hemisphere*, the *southern hemisphere* and the *equator* respectively by $H_+ = \{y \in \mathbb{S}^2 : y_3 > 0\}$, $H_- = \{y \in \mathbb{S}^2 : y_3 < 0\}$ and $\mathbb{S}^1 = \{y \in \mathbb{S}^2 : y_3 = 0\}$.

Consider now the projections $f_{\pm} : \mathbb{R}^2 \rightarrow H_{\pm}$ given by

$$f_{\pm}(x_1, x_2) = \pm \Delta(x_1, x_2)(x_1, x_2, 1),$$

where $\Delta(x_1, x_2) = (x_1^2 + x_2^2 + 1)^{-\frac{1}{2}}$. These two maps define two copies of X , one copy X^+ in H_+ and one copy X^- in H_- . Consider the vector field $X' = X^+ \cup X^-$ defined in $\mathbb{S}^2 \setminus \mathbb{S}^1$. Note that the *infinity* of \mathbb{R}^2 is identified with the equator \mathbb{S}^1 . The Poincaré compactified vector field $p(X)$ is the analytic extension of X' from $\mathbb{S}^2 \setminus \mathbb{S}^1$ to \mathbb{S}^2 given by $y_3^{n-1} X'$. The *Poincaré disk* \mathbb{D} is the projection of the closed northern hemisphere to $y_3 = 0$ under $(y_1, y_2, y_3) \mapsto (y_1, y_2)$ (the vector field given by this projection is also denoted by $p(X)$). Note that to know the behavior $p(X)$ near \mathbb{S}^1 is the same than to know the behavior of X near the infinity. We define the local charts of \mathbb{S}^2 by $U_i = \{y \in \mathbb{S}^2 : y_i > 0\}$ and $V_i = \{y \in \mathbb{S}^2 : y_i < 0\}$ for $i \in \{1, 2, 3\}$. In these charts we define $\phi_i : U_i \rightarrow \mathbb{R}^2$ and $\psi_i : V_i \rightarrow \mathbb{R}^2$ by

$$\phi_i(y_1, y_2, y_3) = -\psi_i(y_1, y_2, y_3) = \left(\frac{y_m}{y_i}, \frac{y_n}{y_i} \right),$$

where $m \neq i$, $n \neq i$ and $m < n$. Denoting by (u, v) the image of ϕ_i and ψ_i in every chart (therefore (u, v) play different roles in each chart) one can see the following expressions for $p(X)$:

$$\begin{aligned} & v^n m(u, v) \left(Q \left(\frac{1}{v}, \frac{u}{v} \right) - uP \left(\frac{1}{v}, \frac{u}{v} \right), -vP \left(\frac{1}{v}, \frac{u}{v} \right) \right) \text{ in } U_1, \\ & v^n m(u, v) \left(P \left(\frac{u}{v}, \frac{1}{v} \right) - uQ \left(\frac{u}{v}, \frac{1}{v} \right), -vQ \left(\frac{u}{v}, \frac{1}{v} \right) \right) \text{ in } U_2, \\ & m(u, v)(P(u, v), Q(u, v)) \text{ in } U_3, \end{aligned}$$

where $m(u, v) = (u^2 + v^2 + 1)^{-\frac{1}{2}(n-1)}$. We can omit the term $m(u, v)$ by a time rescaling of $p(X)$. Therefore, we obtain a polynomial expression of $p(X)$ in each U_i . The expressions of $p(X)$ in each V_i is the same as that for each U_i , except by a multiplicative factor of $(-1)^{n-1}$. In these coordinates for $i \in \{1, 2\}$, $v = 0$ always represents the points of \mathbb{S}^1 and thus the infinity of \mathbb{R}^2 . Note that \mathbb{S}^1 is invariant under the flow of $p(X)$.

APPENDIX C. BLOW UP TECHNIQUE

If the origin is an isolated singularity of a *polynomial* vector field X , then we can apply the change of coordinates $\phi : \mathbb{R}_+ \times \mathbb{S}^1 \rightarrow \mathbb{R}^2$ given by $\phi(\theta, r) = (r \cos \theta, r \sin \theta) = (x, y)$, where $\mathbb{R}_+ = \{r \in \mathbb{R} : r > 0\}$. Therefore, we can induce a vector field X_0 in $\mathbb{R}_+ \times \mathbb{S}^1$ by pullback, i.e. $X_0 = D\phi^{-1}X$. One can see that if the k -jet of X (i.e. the Taylor expansion of order k of X , denoted by j_k) is zero at the origin, then the k -jet of X_0 is also zero in every point of $\{0\} \times \mathbb{S}^1$. Thus, taking the first $k \in \mathbb{N}$ satisfying $j_k(0, 0) = 0$ and $j_{k+1}(0, 0) \neq 0$ we can define the vector field $\hat{X} = \frac{1}{r^k}X_0$. Therefore, to know the behavior of \hat{X} near \mathbb{S}^1 is the same than to know the behavior of X near the origin. One can also see that \mathbb{S}^1 is invariant under the flow of \hat{X} . Observe that \hat{X} is given by

$$\dot{r} = \frac{x\dot{x} + y\dot{y}}{r^{k+1}}, \quad \dot{\theta} = \frac{x\dot{y} - y\dot{x}}{r^{k+2}}.$$

There is a generalization of the Blow Up Technique, known as *Quasihomogeneous Blow Up*, where the change of variables is given by

$$\psi(\theta, r) = (r^\alpha \cos \theta, r^\beta \sin \theta) = (x, y),$$

for $(\alpha, \beta) \in \mathbb{N}^2$. The pair (α, β) is called the *weight* of the quasihomogeneous blow up. Similarly to the previous technique, we can induce a vector field X_0 in $\mathbb{R}_+ \times \mathbb{S}^1$. For some $k \in \mathbb{N}$ maximal one can define $X_{\alpha, \beta} = \frac{1}{r^k}X_0$ and see that this vector field is given by

$$\dot{r} = \xi(\theta) \frac{\cos \theta r^\beta \dot{x} + \sin \theta r^\alpha \dot{y}}{r^{\alpha+\beta+k-1}}, \quad \dot{\theta} = \xi(\theta) \frac{\alpha \cos \theta r^\alpha \dot{y} - \beta \sin \theta r^\beta \dot{x}}{r^{\alpha+\beta+k}},$$

where $\xi(\theta) = (\beta \sin^2 \theta + \alpha \cos^2 \theta)^{-1}$. Observe that the factor $\xi(\theta)$ can be cancel out by time rescaling. Similarly to the previous technique, to know the behavior of $X_{\alpha, \beta}$ near \mathbb{S}^1 (which is invariant) is the same than to know the behavior of X near the origin.

There is another blow up technique, known as *Quasihomogeneous directional Blow Up*. This time we consider the change of coordinates

$$\begin{cases} (x, y) \mapsto (x_1^\alpha, x_1^\beta y_1) & \text{positive } x\text{-direction} \\ (x, y) \mapsto (-x_1^\alpha, x_1^\beta y_1) & \text{negative } x\text{-direction} \\ (x, y) \mapsto (x_1 y_1^\alpha, y_1^\beta) & \text{positive } y\text{-direction} \\ (x, y) \mapsto (x_1 y_1^\alpha, -y_1^\beta) & \text{negative } y\text{-direction,} \end{cases}$$

where $(\alpha, \beta) \in \mathbb{N}^2$. Again the pair (α, β) is called the *weight* of the quasihomogeneous directional blow up. For example, if we do a Quasihomogeneous blow up at the positive x -direction, leading to a vector field X_+^x , then to understand the positive x -direction, i.e. $x > 0$, of X is the same than to understand the positive x_1 -direction of vector field X_+^x . Similarly to the previous techniques, for some $k \in \mathbb{N}$ maximal one can divide X_+^x and X_-^x by x^k (and X_+^y, X_-^y by y^k) and study a regularized version of these systems. Moreover, these vectors fields (not regularized)

are given by

$$\dot{x}_1 = \frac{1}{\alpha} x_1^{1-\alpha} \dot{x}, \quad \dot{y}_1 = \frac{x_1^\alpha \dot{y} - \frac{\beta}{\alpha} \dot{x} y}{x_1^{\alpha+\beta}} \quad \text{at the positive } x\text{-direction,}$$

$$\dot{x}_1 = -\frac{1}{\alpha} x_1^{1-\alpha} \dot{x}, \quad \dot{y}_1 = \frac{x_1^\alpha \dot{y} + \frac{\beta}{\alpha} \dot{x} y}{x_1^{\alpha+\beta}} \quad \text{at the negative } x\text{-direction,}$$

$$\dot{x}_1 = \frac{y_1^\beta \dot{x} - \frac{\alpha}{\beta} \dot{y} x}{y_1^{\alpha+\beta}}, \quad \dot{y}_1 = \frac{1}{\beta} y_1^{1-\beta} \dot{y} \quad \text{at the positive } y\text{-direction,}$$

$$\dot{x}_1 = \frac{y_1^\beta \dot{x} + \frac{\alpha}{\beta} \dot{y} x}{y_1^{\alpha+\beta}}, \quad \dot{y}_1 = -\frac{1}{\beta} y_1^{1-\beta} \dot{y} \quad \text{at the negative } y\text{-direction.}$$

For a more detailed study of the blow up technique we refer to [17, Chapter 3] and [1]. For a nice generalization of this technique in which the infinity is “exploded” instead of the origin, we refer to the recent work [15].

APPENDIX D. MARKUS-NEUMANN THEOREM

Let X be a *polynomial* vector field and $p(X)$ be its compactification defined on \mathbb{D} and ϕ the flow defined by $p(X)$. The separatrices of $p(X)$ are given by the following.

1. All the orbits contained in \mathbb{S}^1 , i.e. at infinity.
2. All the singular points.
3. All the separatrices of the hyperbolic sectors of the finite and infinite singular points.
4. All the limit cycles of X .

Denote by \mathcal{S} the set of all separatrices. It is known that \mathcal{S} is closed, see for instance [17]. Each connected component of $\mathbb{D} \setminus \mathcal{S}$ is called a *canonical region* of the flow (\mathbb{D}, ϕ) . The *separatrix configuration* \mathcal{S}_c of a flow (\mathbb{D}, ϕ) is the union of all the separatrices \mathcal{S} of the flow together with one orbit belonging to each canonical region. The separatrix configuration \mathcal{S}_c of the flow (\mathbb{D}, ϕ) is topologically equivalent to the separatrix configuration \mathcal{S}_c^* of the flow (\mathbb{D}, ϕ^*) if there exists a homeomorphism from \mathbb{D} to \mathbb{D} which transforms orbits of \mathcal{S}_c into orbits of \mathcal{S}_c^* and preserves or reverses the orientation of all these orbits.

Theorem 2 (Markus-Neumann). *Let $p(X)$ and $p(Y)$ be two Poincaré compactifications in the Poincaré disk \mathbb{D} of two polynomial vector fields X and Y with finitely many singularities, respectively. Then the phase portraits of $p(X)$ and $p(Y)$ are topologically equivalent if and only if their separatrix configurations are topologically equivalent.*

For a proof of this theorem see [18, 26, 28]. For a nice digestion of the complete proof we also refer to the recent work [11].

Remark 3. *In Figures 19 to 36 we have written the separatrix configurations of the corresponding Poincaré compactifications.*

APPENDIX E. INDEX OF SINGULARITIES OF A VECTOR FIELD

Let p be an isolated singularity of a *polynomial* vector field X . Let e and h denote the number of elliptical and hyperbolic sectors of p , respectively. The *Poincaré index* of p is given by

$$i_p = \frac{e - h}{2} + 1.$$

It is known that $i_p \in \mathbb{Z}$. See for instance [17, Chapter 6].

Proposition 19. *Let Γ be a limit cycle of a planar polynomial vector field X . Then there is at least one singularity in the bounded region limited by it. Moreover if there is a finite number of singularities in the bounded region limited by Γ , then the sum of their Poincaré indices is 1.*

Theorem 3 (Poincaré-Hopf Theorem). *Let X be a planar polynomial vector field and $p(X)$ its compactification defined on \mathbb{S}^2 . If $p(X)$ has a finite number of singularities, then the sum of their Poincaré indices is 2.*

For a proof of Proposition 19 and Theorem 3 we refer to [17, Chapter 6].

APPENDIX F. THE CARDANO-TARTAGLIA FORMULA

Given a cubic equation

$$(7) \quad x^3 + px + q = 0,$$

if we make the change of variable $x = u + v$ on (7) we obtain

$$u^3 + v^3 + (3uv + p)(u + v) + q = 0.$$

Assuming that $3uv + p = 0$ one obtain $u^3 + v^3 = -q$. The combination of the equations

$$u^3 v^3 = -\frac{1}{27}p^3, \quad u^3 + v^3 = -q$$

imply that u^3 and v^3 are the zeros of

$$z^2 + qz - \frac{1}{27}p^3 = 0.$$

Therefore,

$$u^3 = -\frac{q}{2} + \left(\frac{q^2}{4} + \frac{p^3}{27}\right)^{\frac{1}{2}}, \quad v^3 = -\frac{q}{2} - \left(\frac{q^2}{4} + \frac{p^3}{27}\right)^{\frac{1}{2}}.$$

Remark 4. *We observe that $x^{\frac{1}{n}}$ denotes the standard n th root of x , i.e. if $x = re^{i\theta}$, then $x^{\frac{1}{n}} = \sqrt[n]{r}e^{i\frac{\theta}{n}}$, where $\sqrt[n]{x}$ denotes the n th real root (when it exists) of x . For example, $8^{\frac{1}{3}} = \sqrt[3]{8} = 2$, but $(-8)^{\frac{1}{3}} = 1 + i\sqrt{3}$ while $\sqrt[3]{-8} = -2$. In general both functions coincide when x is a non-negative real number.*

Let $D = \frac{1}{4}q^2 + \frac{1}{27}p^3$ and observe that if $D \geq 0$, then u^3 and v^3 are real numbers and thus we can take

$$\mu = \sqrt[3]{u^3}, \quad \nu = \sqrt[3]{v^3}.$$

Observe that these values do satisfy $\mu^3 + \nu^3 = -q$ and $3\mu\nu + p = 0$. Hence

$$x = \mu + \nu = \sqrt[3]{-\frac{q}{2} + \left(\frac{q^2}{4} + \frac{p^3}{27}\right)^{\frac{1}{2}}} + \sqrt[3]{-\frac{q}{2} - \left(\frac{q^2}{4} + \frac{p^3}{27}\right)^{\frac{1}{2}}}$$

is a (real) solution of (7). Let $\xi = e^{i\frac{\pi}{3}}$ be a root of the unity and observe that the three solutions of (7), when $D \geq 0$, are given by

$$x_k = \xi^k \sqrt[3]{-\frac{q}{2} + \left(\frac{q^2}{4} + \frac{p^3}{27}\right)^{\frac{1}{2}}} + \xi^{2k} \sqrt[3]{-\frac{q}{2} - \left(\frac{q^2}{4} + \frac{p^3}{27}\right)^{\frac{1}{2}}},$$

where $k \in \{0, 1, 2\}$. If $D < 0$ we cannot take any third root of u^3 and v^3 because not every choosing of roots satisfy $3\mu\nu + p = 0$. To satisfy this it is enough that u be the conjugate of v . Therefore we can take

$$\mu = (u^3)^{\frac{1}{3}}, \quad \nu = (v^3)^{\frac{1}{3}}.$$

Hence the solutions of (7) when $D < 0$ are given by

$$x_k = \xi^k \left(-\frac{q}{2} + \left(\frac{q^2}{4} + \frac{p^3}{27}\right)^{\frac{1}{2}}\right)^{\frac{1}{3}} + \xi^{2k} \left(-\frac{q}{2} - \left(\frac{q^2}{4} + \frac{p^3}{27}\right)^{\frac{1}{2}}\right)^{\frac{1}{3}},$$

where $k \in \{0, 1, 2\}$. Observe that if we take these roots when $D \geq 0$, then μ is not necessarily the conjugate of ν (for example if both u^3 and v^3 are negative real numbers) and thus we would not have a solution of (7). At the other hand, we cannot always apply the $\sqrt[3]{\cdot}$ when $D < 0$ because not every complex number has a third real root.

If we denote by S and T the *convenient root* of u^3 and v^3 (i.e. denotes the root according to the logic of this section), respectively, then the solutions of (7) are given by

$$\begin{cases} x_1 = S + T. \\ x_2 = -\frac{1}{2}(S + T) + \frac{1}{2}\sqrt{3}(S - T)i. \\ x_3 = -\frac{1}{2}(S + T) - \frac{1}{2}\sqrt{3}(S - T)i. \end{cases}$$

One can see that if $D < 0$, then all solutions are real and simple. If $D = 0$ and $q \neq 0$, then x_1 is a real simple solution and $x_2 = x_3$ is a double real solution. If $D = q = 0$, then $x_1 = x_2 = x_3$ is a real triple solution. Finally if $D > 0$, then x_1 is a real simple solution and x_2, x_3 are two complex conjugates solutions.

REFERENCES

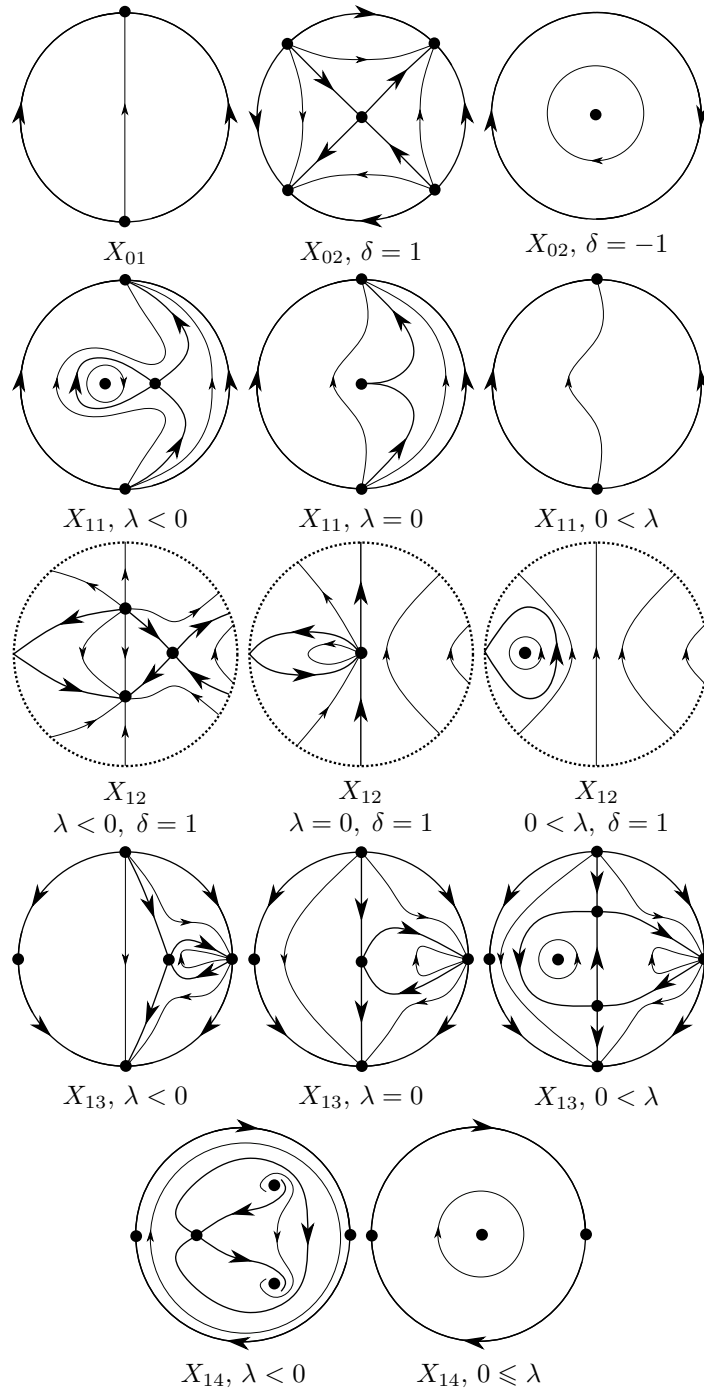
- [1] M. J. ALVAREZ, A. FERRAGUT AND X. JARQUE, *A survey on the blow up technique*, Int. J. Bifurcation Chaos Appl. Sci. Eng. 21, No. 11, 3103-3118 (2011).
- [2] J. C. ARTES AND J. LLIBRE, *Quadratic Hamiltonian vector fields*, J. Differ. Equations 107, No. 1, 80-95 (1994).
- [3] J. C. ARTES AND J. LLIBRE, *A correction to the paper "Quadratic Hamiltonian vector fields"*, J. Differ. Equations 129, No. 2, 559-560 (1996).
- [4] J. C. ARTES, R. E. KOOLJ AND J. LLIBRE, *Structurally stable quadratic vector fields*, Mem. Am. Math. Soc. 639, 108 p. (1998).
- [5] J. C. ARTES, J. LLIBRE AND A. C. REZENDE, *Structurally unstable quadratic vector fields of codimension one*, Cham: Birkhäuser. VI, 267 p. (2018).
- [6] J. C. ARTES, M. MOTA AND A. C. REZENDE, *Structurally unstable quadratic vector fields of codimension two: families possessing a finite saddle-node and an infinite saddle-node*, Electron. J. Qual. Theory Differ. Equ. 2021, Paper No. 35, 89 p. (2021).
- [7] J. C. ARTES, R. D. S OLIVEIRA AND A. C. REZENDE, *Structurally unstable quadratic vector fields of codimension two: families possessing either a cusp point or two finite saddle-nodes*, J. Dyn. Differ. Equations 33, No. 4, 1779-1821 (2021).
- [8] J. C. ARTES, *Structurally unstable quadratic vector fields of codimension two: families possessing one finite saddle-node and a separatrix connection*, Qual. Theory Dyn. Syst. 23, No. 1, Paper No. 40, 88 p. (2024).

- [9] J. C. ARTES, J. LLIBRE, D. SCHLOMIUK AND N. VULPE, *Invariant conditions for phase portraits of quadratic systems with complex conjugate invariant lines meeting at a finite point*, Rend. Circ. Mat. Palermo (2) 70, no. 2, 923–945. (2021).
- [10] J. C. ARTES, L. CAIRO AND J. LLIBRE, *Phase Portraits of the Family IV of the Quadratic Polynomial Differential Systems*, Qual. Theory Dyn. Syst. 24 (2025), no. 2, Paper No. 66.
- [11] F. BRAUN AND R. THOMAZ, *Revisiting Markus–Neumann theorem*, São Paulo J. Math. Sci. 19, No. 1, Paper No. 8, 33 p. (2025).
- [12] C. A. BUZZI, *Generic one-parameter families of reversible vector fields*, Bruce, J. W. (ed.) et al., Real and complex singularities. Proceedings of the 5th workshop, São Carlos, Brazil, July 27–31, 1998. Boca Raton, FL: Chapman & Hall/CRC. Chapman Hall/CRC Res. Notes Math. 412, 202–214 (2000).
- [13] C. A. BUZZI, J. LLIBRE AND P. SANTANA, *Phase portraits of $(2;0)$ reversible vector fields with symmetrical singularities*, J. Math. Anal. Appl. 503, No. 2, Article ID 125324, 21 p. (2021).
- [14] L. CAIRO AND J. LLIBRE, *Phase Portraits of Families VII and VIII of the Quadratic Systems*, Axioms, 12(8), 756. (2023).
- [15] T. M. DALBELO, R. OLIVEIRA AND O. H. PEREZ, *Topological equivalence at infinity of a planar vector field and its principal part defined through Newton polytope*, J. Differ. Equations 408, 230–253 (2024).
- [16] L. E. DICKSON, *Elementary Theory of Equations*, New York: John Wiley and Sons. V + 184 S. (1914).
- [17] F. DUMORTIER, J. LLIBRE AND J. C. ARTES, *Qualitative theory of planar differential systems*, Universitext, Berlin: Springer. xvi, 298 p. (2006).
- [18] J. G. ESPIN BUENDIA AND V. JIMENEZ LOPEZ, *On the Markus–Neumann theorem*, J. Differ. Equations 265, No. 11, 6036–6047 (2018).
- [19] A. GASULL, H. GIACOMINI AND J. TORREGROSA, *Some results on homoclinic and heteroclinic connections in planar systems*, Nonlinearity 23, No. 12, 2977–3001 (2010).
- [20] M. R. A. GOUVEIA, J. LLIBRE AND L. A. ROBERTO, *Phase portraits of the quadratic polynomial Liénard differential systems*, Proc. R. Soc. Edinb., Sect. A, Math. 151, No. 1, 202–216 (2021).
- [21] M. W. HIRSCH, S. SMALE AND R. L. DEVANEY, *Differential equations, dynamical systems, and an introduction to chaos. 2nd ed*, Pure Appl. Math., Amst. 60. xiv, 417 p. (2004).
- [22] J. LLIBRE, B. D. LOPES AND P. R. DA SILVA, *Bifurcations of the Riccati quadratic polynomial differential systems*, Int. J. Bifurcation Chaos Appl. Sci. Eng. 31, No. 6, Article ID 2150094, 13 p. (2021).
- [23] J. LLIBRE AND J. MEDRADO, *Darboux Integrability and Reversible Quadratic Vector Fields*, Rocky Mt. J. Math. 35, No. 6, 1999–2057 (2005).
- [24] J. LLIBRE, W. F. PEREIRA AND C. PESSOA, *Phase portraits of Bernoulli quadratic polynomial differential systems*, Electron. J. Differ. Equ. 2020, Paper No. 48, 19 p. (2020).
- [25] J. LLIBRE AND C. VALLS, *Global phase portraits of quadratic systems with a complex ellipse as invariant algebraic curve*, Acta Math. Sin., Engl. Ser. 34, No. 5, 801–811 (2018).
- [26] L. MARKUS, *Global structure of ordinary differential equations in the plane*, Trans. Am. Math. Soc. 76, 127–148 (1954).
- [27] J. MEDRADO AND M. A. TEIXEIRA, *Symmetric singularities of reversible vector fields in dimension three*, Physica D 112, No. 1–2, 122–131 (1998).
- [28] D. A. NEUMANN, *Classification of continuous flows on 2-manifolds*, Proc. Am. Math. Soc. 48, 73–81 (1975).
- [29] W. F. PEREIRA AND C. PESSOA, *A class of reversible quadratic polynomial vector fields on S^2* , J. Math. Anal. Appl. 371, No. 1, 203–209 (2010).
- [30] W. F. PEREIRA AND C. PESSOA, *On the reversible quadratic polynomial vector fields on S^2* , J. Math. Anal. Appl. 396, No. 2, 455–465 (2012).
- [31] L. M. PERKO, *Differential equations and dynamical systems. 3rd ed*, Texts Appl. Math. 7. xiv, 553 p. (2001).
- [32] L. M. PERKO, *Homoclinic loop and multiple limit cycle bifurcation surfaces*, Trans. Am. Math. Soc. 344, No. 1, 101–130 (1994).
- [33] R. K. GEORGE AND A. AJAYAKUMAR, *A course in linear algebra*, Univ. Texts Math. Sci. Singapore: Springer. xiii, 551 p. (2024).
- [34] E. L. REES, *Graphical Discussion of the Roots of a Quartic Equation*, American Math. Monthly 29, 51–55 (1922).

- [35] L. ROBERTO, P. R. DA SILVA AND J. TORREGROSA, *Asymptotic expansion of the heteroclinic bifurcation for the planar normal form of the 1:2 resonance*, Int. J. Bifurcation Chaos Appl. Sci. Eng. 26, No. 1, Article ID 1650017, 8 p. (2016).
- [36] M. A. TEIXEIRA, *Singularities of reversible vector fields*, Physica D 100, No. 1-4, 101-118 (1997).
- [37] M. A. TEIXEIRA, *Generic bifurcation of reversible vector fields on a 2-dimensional manifold*, Publ. Mat., Barc. 41, No. 1, 297-316 (1997).

¹ IBILCE-UNESP, CEP 15054-000, S. J. RIO PRETO, SÃO PAULO, BRAZIL
Email address: `claudio.buzzi@unesp.br`; `paulo.santana@unesp.br`

² UNIVERSITAT AUTÒNOMA DE BARCELONA, 08193 BELLATERRA, BARCELONA, SPAIN
Email address: `jaume.llibre@uab.cat`

FIGURE 19. Phase portraits of X_{01} , X_{02} , X_{11} , X_{12} , X_{13} and X_{14} .

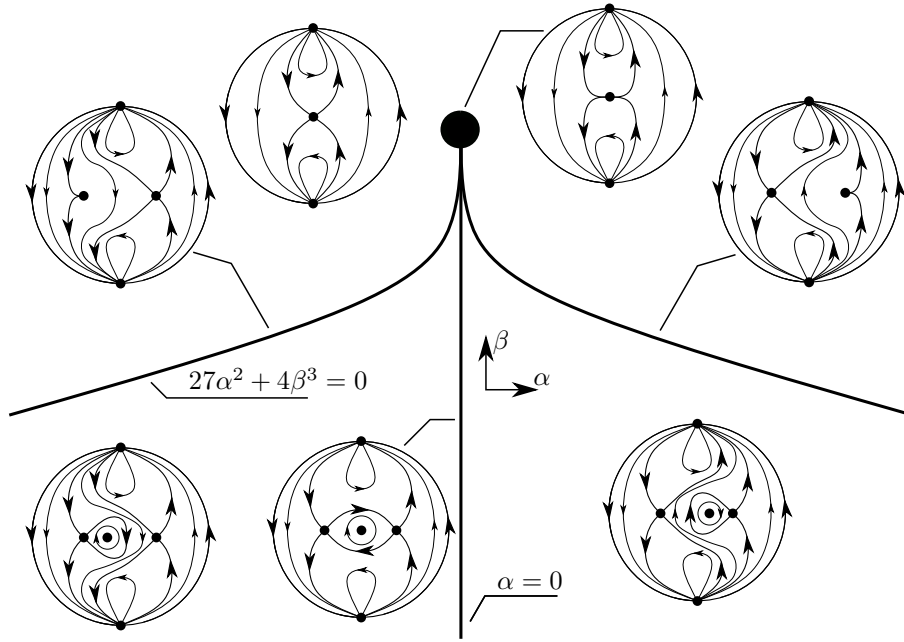


FIGURE 20. Phase portrait of X_{21} with $b = 1$.

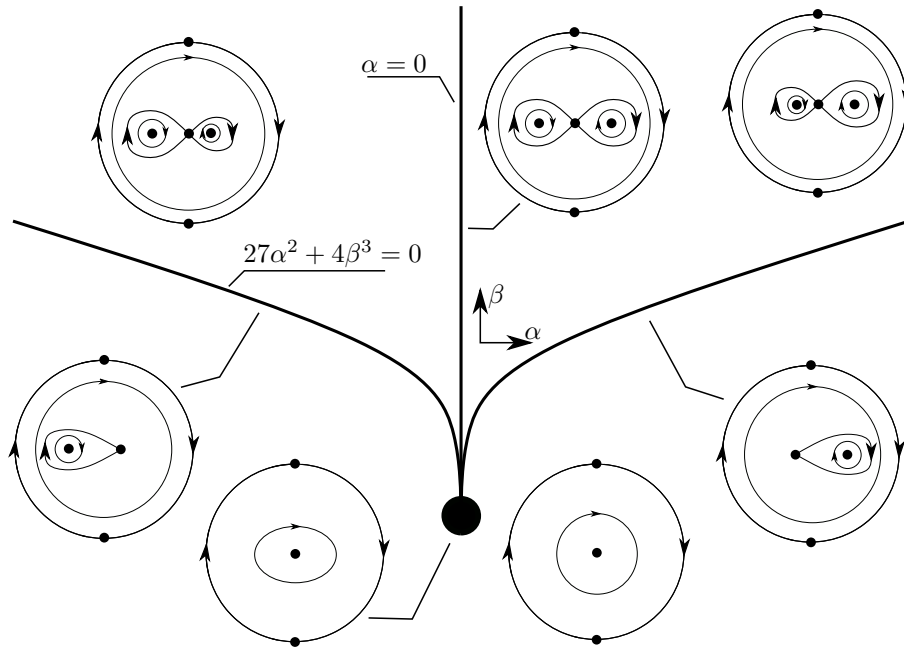
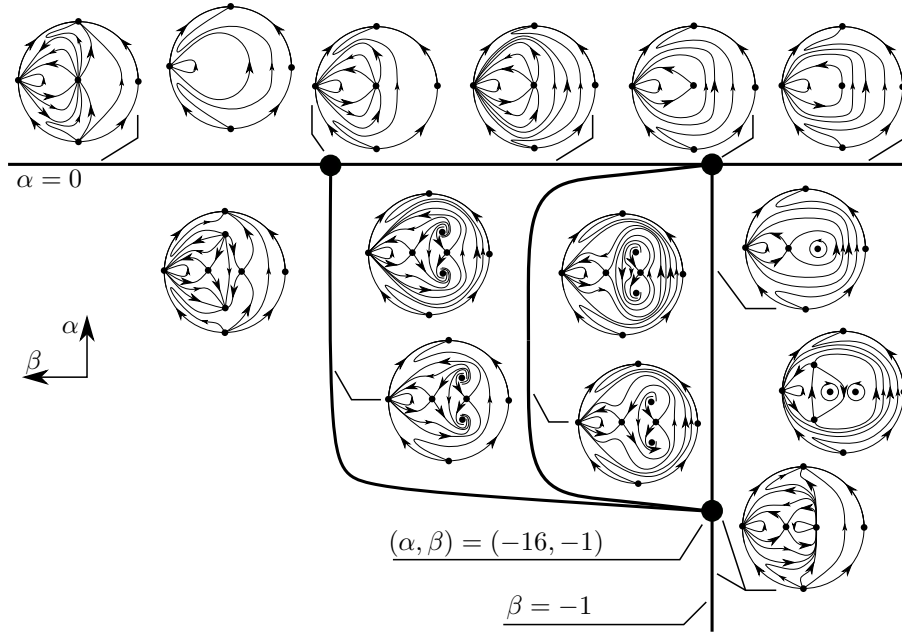
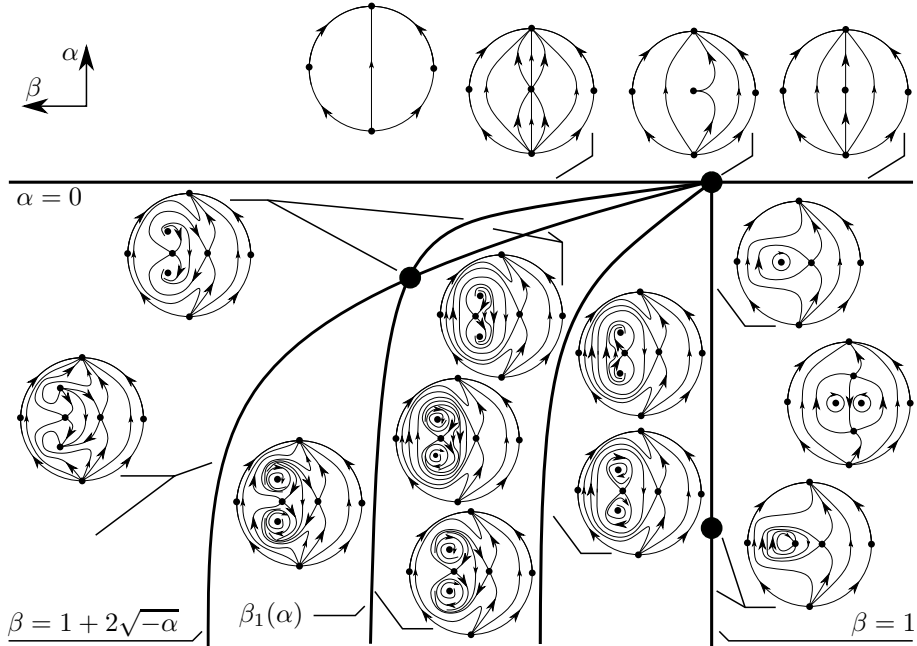


FIGURE 21. Bifurcation diagram of X_{21} with $b = -1$.

FIGURE 22. Bifurcation diagram of X_{22a} with $a = 1$.FIGURE 23. Bifurcation diagram of X_{22a} with $a = -1$.

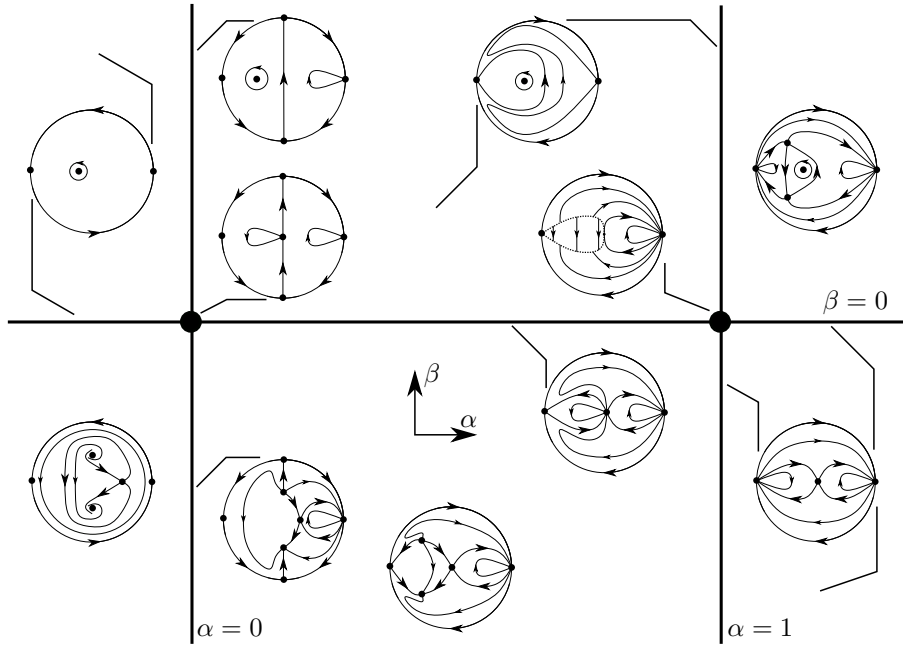


FIGURE 24. Bifurcation diagram of X_{24a} with $a = 1$.

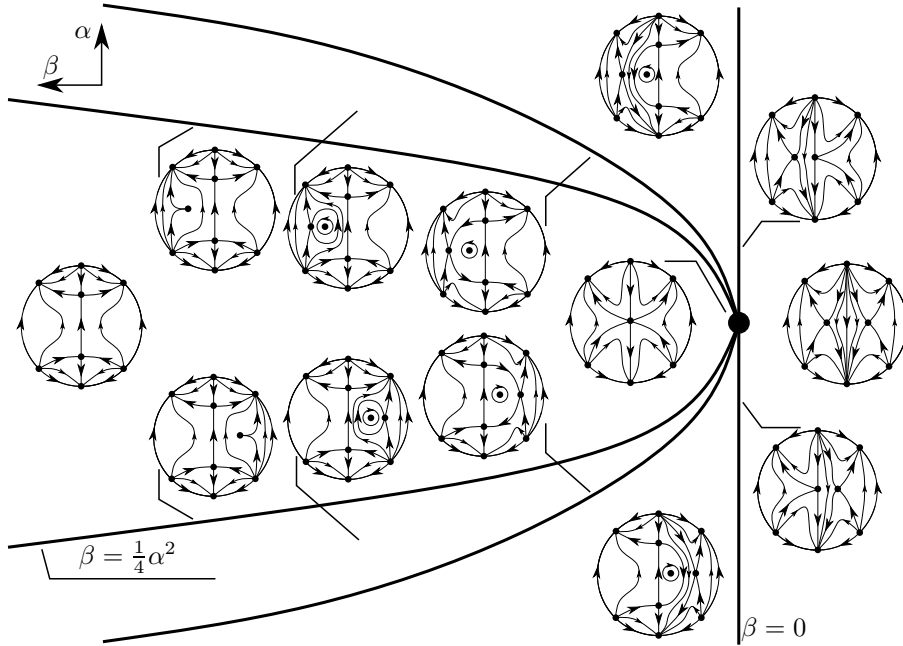
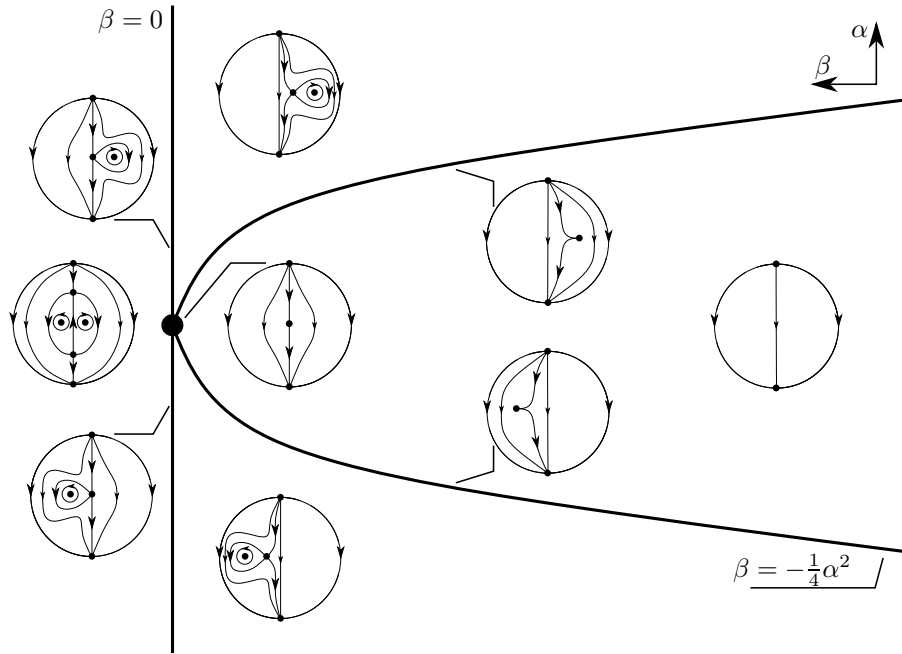
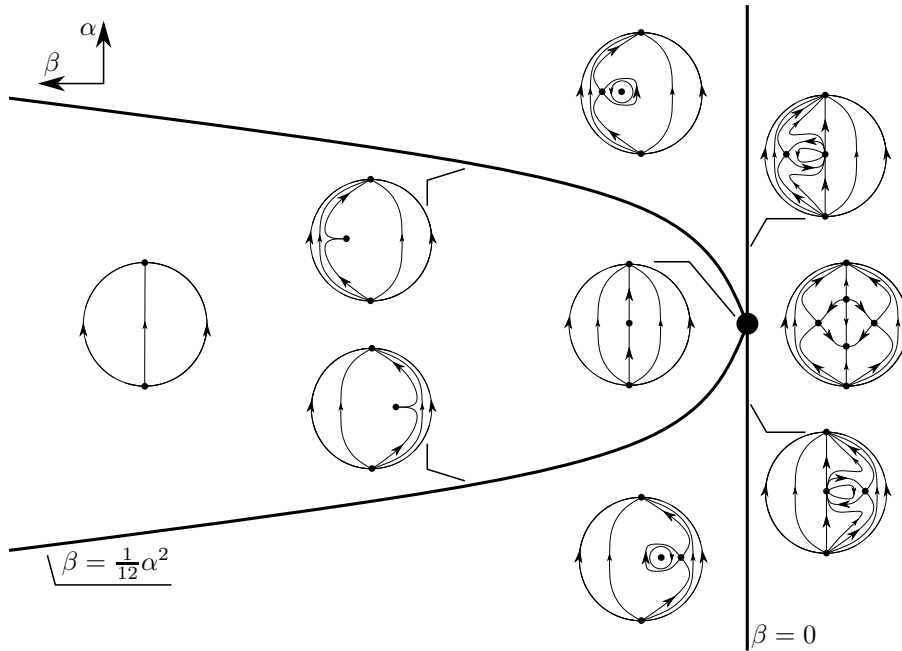


FIGURE 25. Bifurcation diagram of X_{25a} with $a = 1$.

FIGURE 26. Bifurcation diagram of X_{25a} with $a = -1$.FIGURE 27. Bifurcation diagram of X_{25b} with $(a, b, \delta) = (1, 3, 3)$.

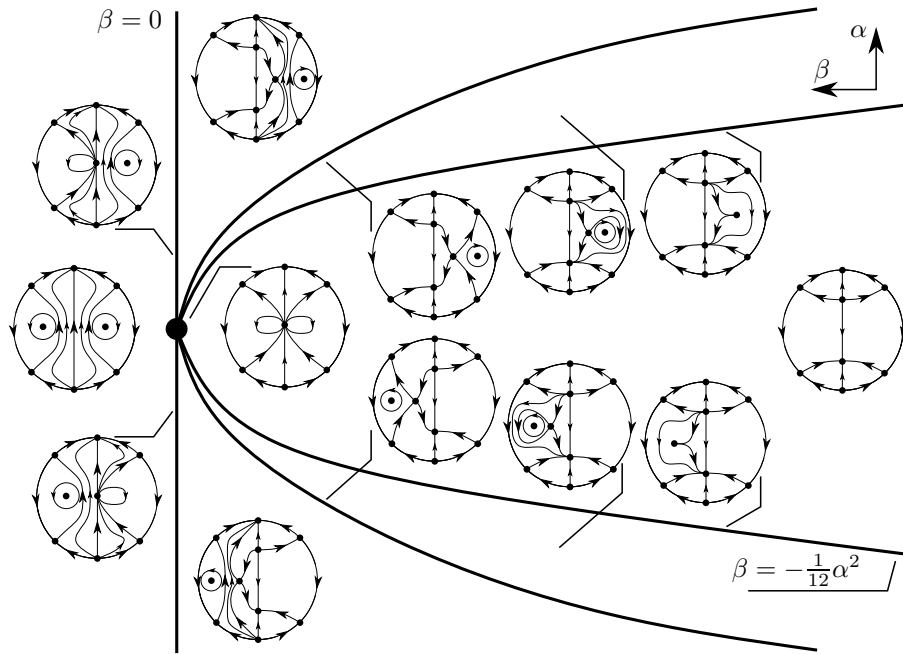


FIGURE 28. Bifurcation diagram of X_{25b} with $(a, b, \delta) = (1, 3, -3)$.

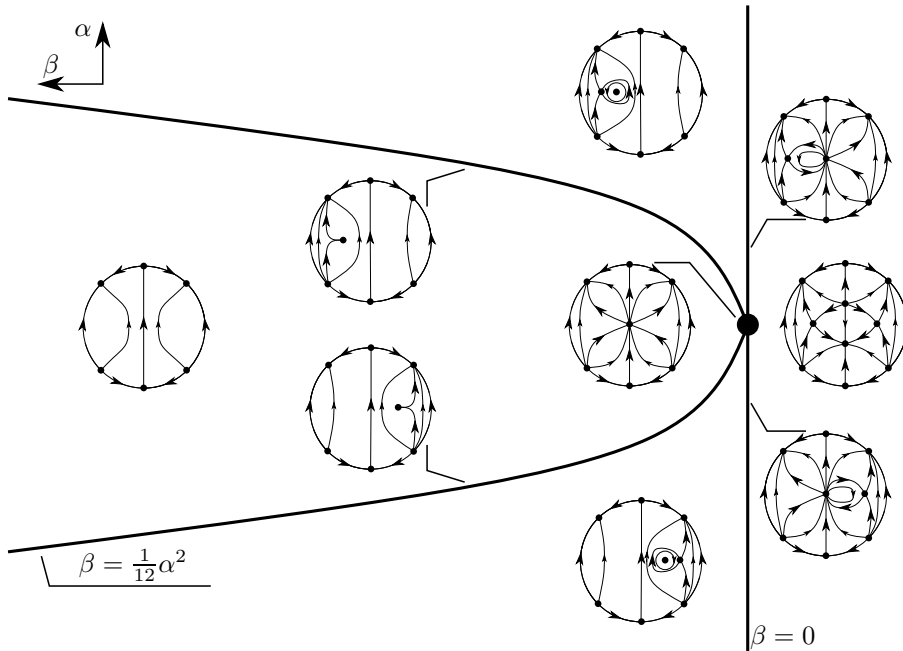


FIGURE 29. Bifurcation diagram of X_{25b} with $(a, b, \delta) = (3, 1, 3)$.

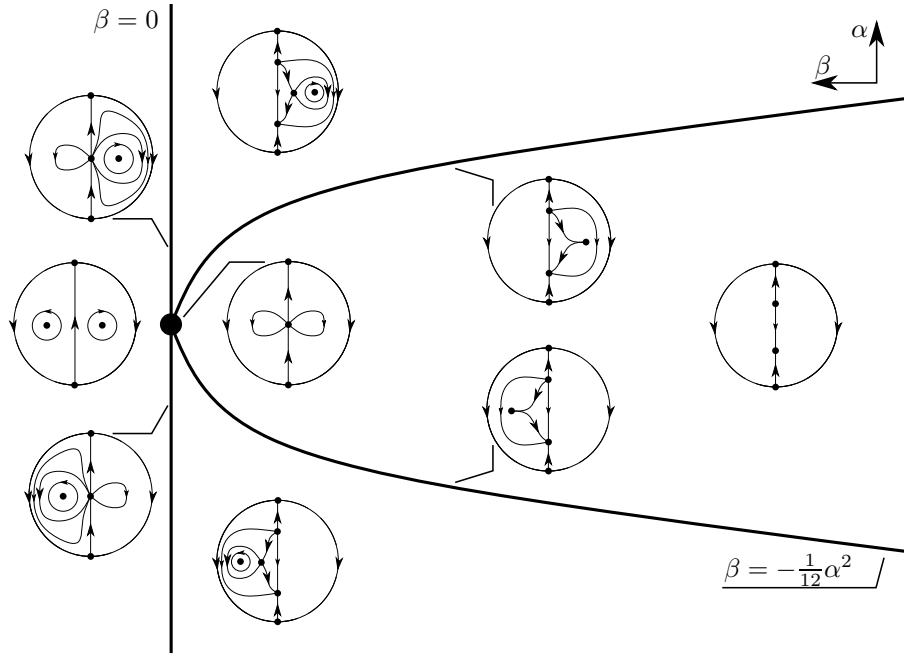


FIGURE 30. Bifurcation diagram of X_{25b} with $(a, b, \delta) = (3, 1, -3)$.

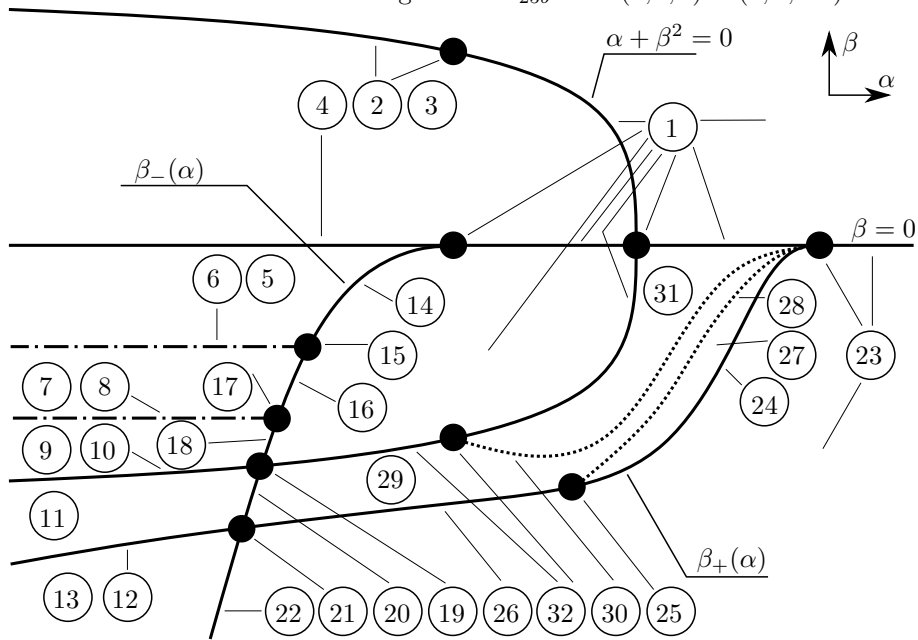


FIGURE 31. Bifurcation diagram of X_{23} with $a = 1$. We observe that it may be an intersection between the dotted lines defined by phase portraits 28 and 30. This is an open problem.

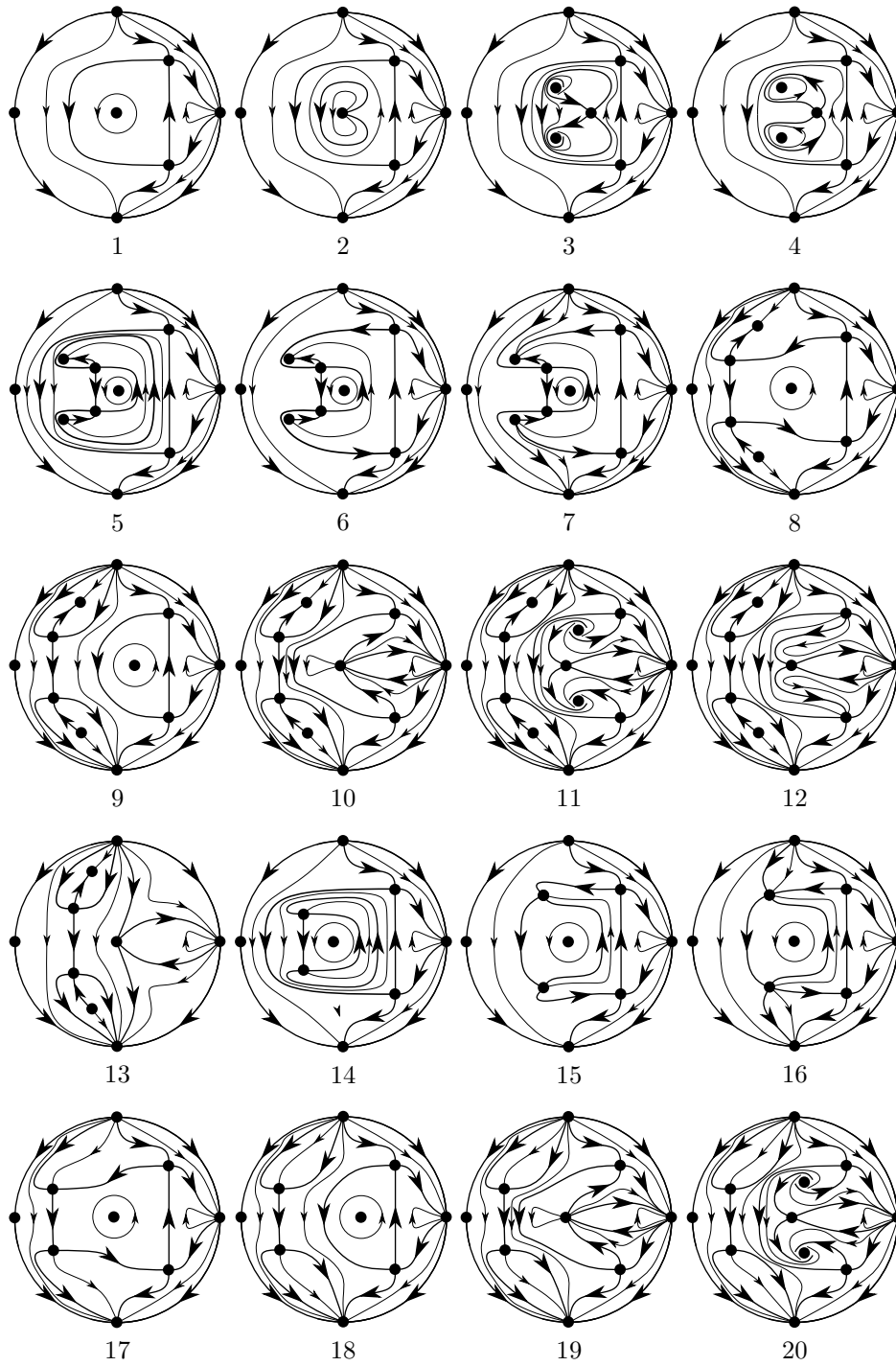


FIGURE 32. Phase portraits of X_{23a} with $a = 1$.

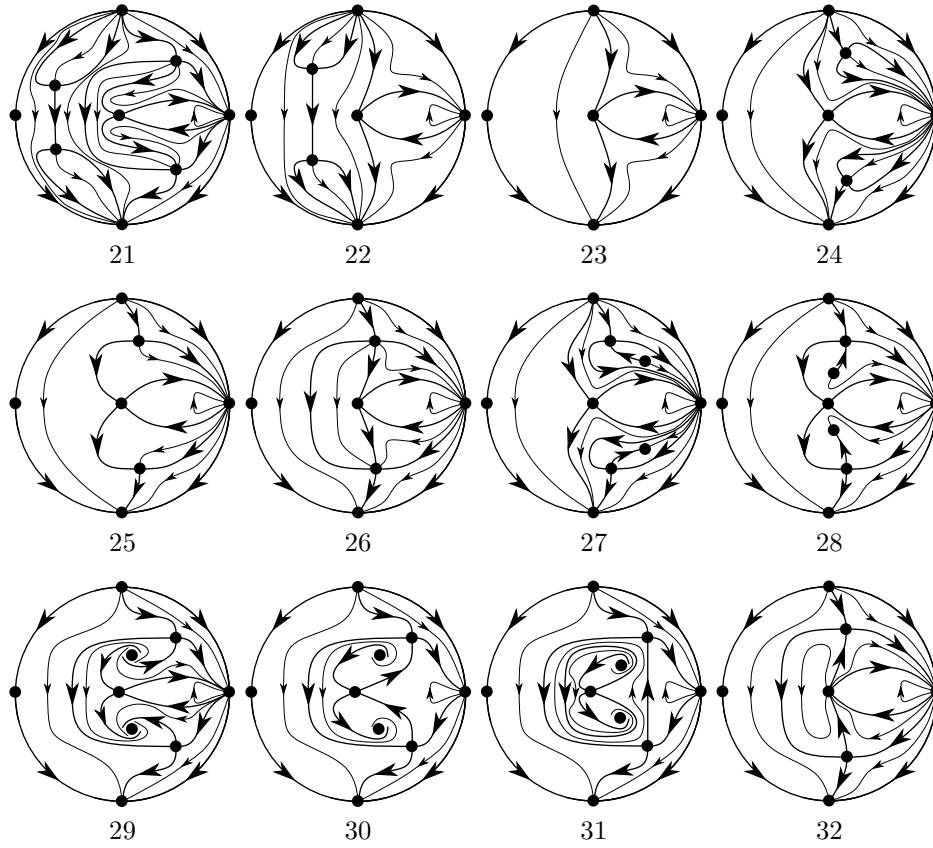


FIGURE 33. Phase portraits of X_{23a} with $a = 1$.

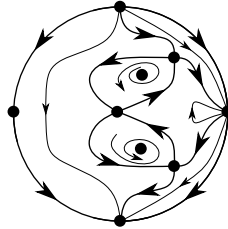


FIGURE 34. We do not know if the dotted lines defined by phase portraits 28 and 30 of Figure 31 intersect each other. But if it happens, then this is the phase portrait on the intersection.

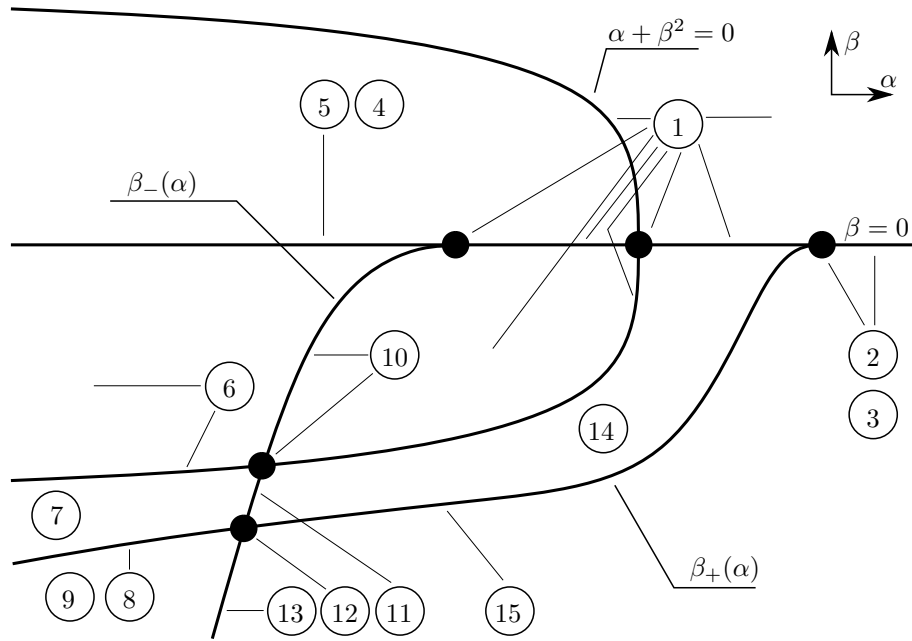


FIGURE 35. Bifurcation diagram of X_{23b} with $a = -1$.

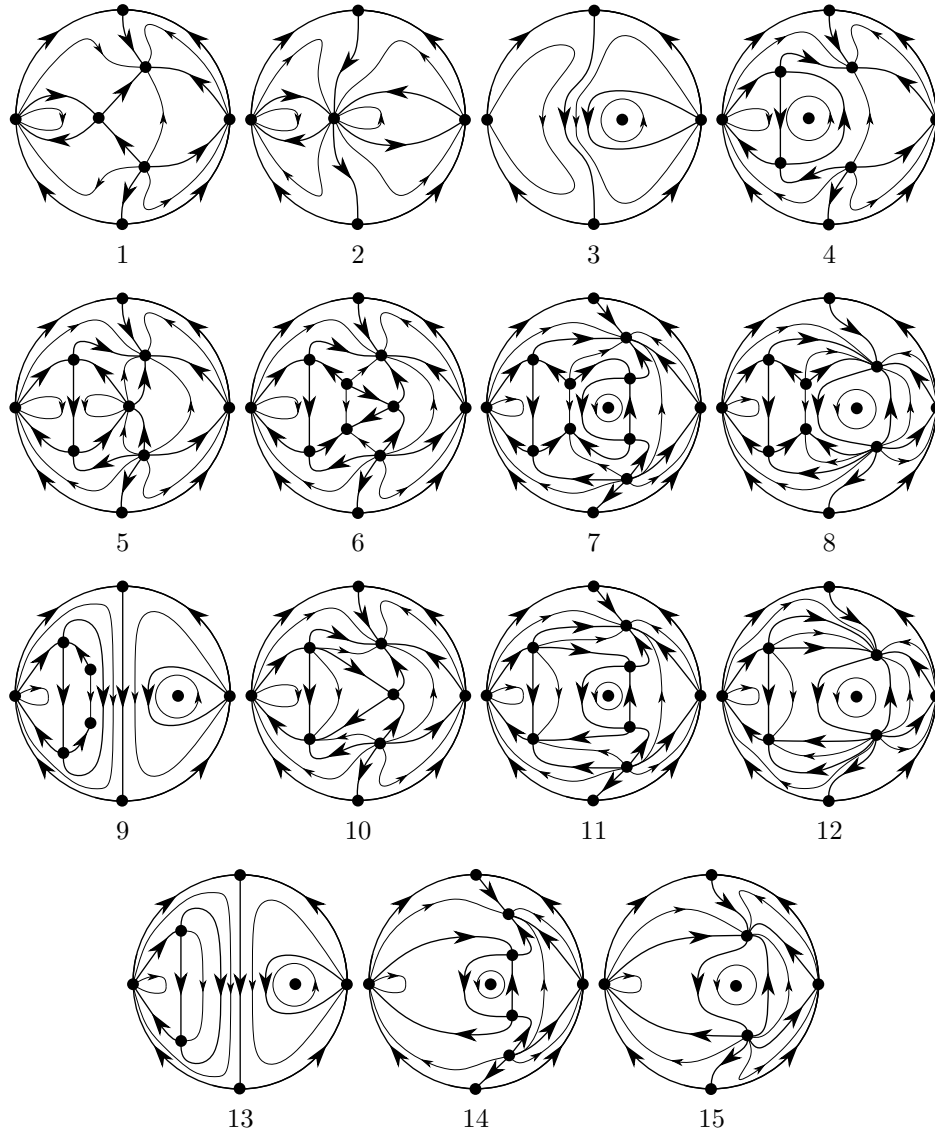


FIGURE 36. Phase portraits of X_{23} with $a = -1$ and $(x, y) \mapsto (-x, y)$.